

2P

U N I V E R S I T E T E T I B E R G E N  
G E O F Y S I S K I N S T I T U T T



Report on Study of Variability  
in the Norwegian Sea April/May 1967

By

Thor Kvinge, Arthur J. Lee, Roald Sætre

BERGEN 1968

UNIVERSITETET I BERGEN

GEOFYSISK INSTITUTT

Report on study of Variability  
in the Norwegian Sea April/May 1967

by

Thor Kvinge, Geophysical Institute, Bergen  
Arthur J. Lee, Fisheries Laboratory, Lowestoft  
Roald Sætre, Geophysical Institute, Bergen

Bergen 1968

## CONTENTS

	Page:
Foreword .....	1
Introduction .....	4
The Observations .....	5
Prevailing Weather Systems .....	7
Bottom Topography .....	9
The Hydrographic Sections .....	10
General Description of the Current Systems in the Norwegian Sea .....	12
The Current Conditions .....	14
Geostrophic Current .....	18
Geostrophic Mass Transport .....	20
Discussion .....	21
Vertical Oscillations .....	25
Final Remarks .....	27
References .....	29
Table I .....	30
Table II .....	31
Figures	

## FOREWORD

Studies of the hydrographic conditions along standard sections have been carried out in the Norwegian Sea for many years. The most notable of these sections is probably the Sognefjord Section Helland-Hansen (1934) reported on early investigations of it, and more recently Sælen (1959 and 1963) has examined in detail the changes in volume transport across it and has discussed possible causes of the pronounced waviness in the isotherms and isohalines which is found in the temperature and salinity distributions whenever it, or any other section in the Norwegian Sea, is worked.

As a result of these and other investigations it has become apparent to Norwegian and British workers over the last few years that, in order to make further progress in the study of the variability of the temperature and salinity conditions in the Norwegian Sea, use must be made of the moored recording instruments which are now becoming available.

Interest in the study of the physical variability of the oceans has also been growing rapidly recently in many other quarters. The Hydrography Committee of the International Council for the Exploration of the Sea (ICES) has paid increasing attention to it at the annual meetings of the Council and has set up a working group on the subject. Further, ICES intends to hold a symposium on the "Physical Variability of the North Atlantic Ocean and its adjacent seas" at Dublin in September 1969. The Intergovernmental Oceanographic Commission (IOC) also has a working group on the same subject and one of its scientific advisory bodies, the Scientific Committee on Oceanic Research (SCOR) held a symposium on Variability in the Ocean in Rome in

May 1966. In order to encourage the development of the necessary recording instrumentation for the study of variability SCOR has established a Working Group on Continuous Velocity Measurements.

It was against this background that scientists at the Geophysical Institute, Bergen and the Fisheries Laboratory, Lowestoft, decided to mount their 1967 study of physical variability of the Norwegian Sea which forms the subject of this report. Its aim was the repeated working over a period of 2 months of a single hydrographic section along which buoys with recording instrumentation had been moored.

In presenting a report on this study at this time it is our intention to make known the first results and to release the whole of the processed data. We feel that it is proper to do this at an early date after the completion of the work at sea rather than to withhold them until we had written a complete and detailed report, a task which might take four or five years. The processed data are held by the institutions listed below and are available on request. It is our hope that other workers will use them to investigate particular topics. For example, our colleague G. Bøyum is already using some of them in connexion with an air-sea interaction study. We ourselves hope at a later date to carry out the power spectrum and tidal analyses of the current measurements.

We thank the many colleagues who made the investigation possible by assisting in the preparation of the instrumentation, in carrying out the research cruises and in the processing of the data. In particular, we would like to thank Ferris Webster of the Woods Hole Oceanographic Institution for his kind assistance in the computer analysis of the current meter data.

Institutions holding data from the 1967 Study of  
Variability in the Norwegian Sea

Geophysical Institute, Bergen, Norway: Temperature and salinity data both as print out and on punched cards (ICES format). Current meter data both as print out and on punched cards. Meteorological data in manuscript form.

Fisheries Laboratory, Lowestoft, England: Temperature and salinity data as print out, but not data for Ocean Weather Station METRO. Print out of derived data. ( $\sigma_t$  specific volume anomaly, dynamic height anomaly, potential energy anomaly, geostrophic current and mass transport). Surface thermograph, GEK and bathythermograph records; all in analogue form.

Woods Hole Oceanographic Institution, Woods Hole, Mass., U.S.A.: Current meter data as print out and on punched cards.

## INTRODUCTION

During April-May 1967 a variability study on hydrographic parameters was carried out in the Norwegian Sea by the Geophysical Institute, Bergen, and Fisheries Laboratory, Lowestoft. Participating ships were: R.V. "H.U. Sverdrup" and R.V. "Helland-Hansen" and R.V. "Ernest Holt".

The observations were taken along the  $66^{\circ}\text{N}$  parallel from  $6^{\circ}\text{E}$  to  $2^{\circ}\text{W}$ , thus passing through the position of Ocean Weather Station METRO where hydrographic stations have been taken since 1948 (Fig. 1). The investigations were concentrated in the Atlantic Water and mainly concerned with periodical variations between 4 hours to 30 days duration.

## THE OBSERVATIONS

Anchored buoys carrying recording current meters (Aanderaa, 1964) were placed in the following positions during the period 1-5 April by R.V. "H.U. Sverdrup":

Station	Position	Sounding	Observation Depth
A	66°03'N 5°20'E	750 m	200 m
B	65°59'N 4°18'E	1300 m	200 m
C	66°01'N 2°04'E	1980 m	200 m and 350 m
D	66°00'N 1°35'E	2500 m	350 m

The positions of the current meters along the section are shown in Figure 2a.

The buoys were lifted for servicing on 21-22 April and finally recovered by R.V. "Helland-Hansen" on 20-22 May.

The current meters recorded integrated current speed over 30 minute intervals and current direction and temperature at the beginning and end of each interval.

Due to instrumental failure, at Station C at 200 m there are no current speed registrations after 23 April. The instrument placed at 350 m at Station C was lost, probably during launching, and consequently there are no observations from this location. The rest of the recording instruments worked perfectly during the periods concerned, giving the following amount of data:

Station	Observation depth	Number of data	Length of observation period
A	200 m	2278	47 days 11 hours
B	200 m	2109	43 days 22½ hours
C	200 m: speed direction and temperature	864 2249	18 days 7½ hours 46 days 20½ hours
C	350 m	No observations	
D	350 m	2194	45 days 17 hours



The hydrographic stations were worked at fixed positions at about 10 n.miles intervals along a section 190 n.miles long between  $6^{\circ}\text{E}$  and  $2^{\circ}\text{W}$ . Temperature and salinity were sampled at the following depths: 0, 50, 100, 150, 200, 300, 400, 500, 600, 700, 800 and 1000 m. A total number of 352 stations were taken, covering altogether 17 crossings of the section. The details of the crossings are given in Table 1 and shown in time sequence in Figure 2b. It should be noted that the hydrographic stations are numbered 1-20 from east to west in contradistinction to the buoy stations which are lettered A-D.

During crossings Nos. 2 and 4, GEK was used. Aboard R.V. "Ernest Holt" a sea surface thermograph was run continuously and at all stations a bathythermograph was lowered to 275 m.

Near buoy Station C ( $66^{\circ}\text{N}$ ,  $-2^{\circ}\text{E}$ ), Nansen bottle casts were taken at 1 hour intervals during 24 hours on 20-21 May.

Meteorological observations were made at hourly intervals whenever a research vessel was within the vicinity of the section.

Ocean Weather Station METRO was occupied by the Weather Ships "Polarfront I" and "Polarfront II" taking hydrographical and meteorological observations according to their normal programme as shown in Table 2.

The section is in an area of good Loran A coverage and the positions of the research vessels could be fixed with an accuracy of  $\pm 0.1$  n.mile.

## PREVAILING WEATHER SYSTEMS

The daily mean north and east components of the winds recorded at Ocean Weather Station METRO for the period 29 March - 20 May are given in Figure 25.

During the few days immediately before the buoy stations were laid there was a depression, low (A), to the southeast of METRO and on 27 March winds there were northeasterly and reached 40 knots. This depression moved to the Barents Sea and winds at METRO decreased to 5 knots, but on 28 March a new low (B) developed to the south of METRO and moved northeastwards giving north to northwest winds at METRO of 35-45 knots. By 1 April these winds had moderated to 20 knots as the depression moved northwards, but a new low (C) was developing south of Iceland. On 2 April low C was to the east of Iceland with winds at METRO in the southeast quadrant and reaching 48 knots, and by 3 April it was to the northwest of METRO with winds there southerly and 30 knots. Low C continued to move northwards and fill, but by 4 April low D was developing to the south of Iceland and moving quickly eastwards. This gave rise to north to northeast winds of 30 knots at METRO on 5 and 6 April.

By 7 April, however, a ridge of high pressure running northeast-southwest was established over METRO and winds there became northeasterly, 18 knots at first and then easterly, less than 10 knots, on 8 and 9 April. The ridge finally drifted southeastwards allowing a series of small depressions to pass through the Denmark Strait, and these gave rise to southwesterly winds reaching 20-35 knots at METRO on 11-15 April. Even stronger winds, westerly at 38 knots, occurred on 15 April when one of these depressions moved to the north of METRO, but this low weakened on 16 April. However, by this time low E was developing to the south of METRO and moving eastwards to give northerly winds of 33 knots on 18 April. On 19 April low F was south of

Iceland and this too moved eastwards to reach the Baltic on 21 April. At the same time a high pressure area developed over Greenland and the western part of the Norwegian Sea. Hence, winds at METRO were in the northeast quadrant at 20-30 knots until 23 April.

On 24 April low G was southwest of Iceland and pressure was high over southern Scandinavia. Winds at METRO became southerly at 42 knots. Low G moved northwards, but low H developed in the Denmark Strait on 25 April and moved to a position northwest of METRO on 27 April, so that winds there were southwesterly at 30 knots on 25-27 April. On 27 April low I was developing over Iceland and it moved northeastwards, giving westerly 30 knots winds at METRO.

On 30 April a change occurred. Pressure became high over Greenland and low over northern Scotland, so that winds at METRO became northerly, 15 knots. The low pressure area moved to southern Scandinavia and remain there until 3 May, with winds at METRO in the northeast quadrant, 20-30 knots. On 4 May a large depression (low J) was situated just west of the British Isles and pressure was high from Greenland to Scandinavia. Winds became easterly, 15-20 knots, at METRO and remained so until 8 May. By 9 May low J had filled and drifted to the Faroes region where it persisted until 11 May: winds at METRO became southeasterly, 10-15 knots, and then northeasterly, less than 10 knots. A ridge of high pressure extended from the Azores to METRO on 12 May and the next day a weak low developed over southern Scandinavia and the Baltic, so that winds at METRO were in the northwest-northeast quadrant, 10-15 knots. On 15 May a high pressure area became established over the southern Norwegian Sea and a low pressure area (low K) over the British Isles. As low K moved towards southern Scandinavia on 16 May, winds at METRO changed from westerly, 12 knots to northerly, 20 to 30 knots. Low K then proceeded to move slowly northwestwards and by 19 and 20 May was positioned northeastwards of METRO: winds changed from northwesterly, 10-20 knots, on 17 May to westerly, 8-34 knots, on 19 May and to southwesterly, 20 knots, on 20 May.

## BOTTOM TOPOGRAPHY

The bottom topography along the section is shown in Figure 2a. It is derived from echo sounder records obtained from R.V. "Ernest Holt" on one of its crossings. It can be seen that the section crossed the continental slope and started at about 500 m depth in the east and reached 3400 m depth in the west. There is a break in the slope between  $2^{\circ}30'E$  and  $4^{\circ}E$  (Stations 6-10) at 1400 m depth. Buoy Stations A and B were situated to the east of this break and buoy Stations C and D immediately west of it. Beyond the break the slope falls rapidly towards the abyssal zone at 3000 m depth and Station D is close to this zone.

## THE HYDROGRAPHIC SECTIONS

The temperature and salinity conditions are subject to great variations with respect to space and time. In the mean stations, however, short periodic or random fluctuations are eliminated by the process of averaging the depth of the isolines. The mean stations and the sections therefore show the stationary or the quasistationary part of the field.

It may furthermore be shown from the mean sections, as well as from those based on single stations, that the isotherms coincide very closely with the isohalines. The most conspicuous and characteristic features may therefore be illustrated by considering the isotherm distribution through a mean section (Fig. 4).

The western side of the section shows admixture of Arctic water, probably related to a tongue of the East Iceland Arctic Current. (Helland-Hansen and Nansen 1909). The magnitude of the intruding water varies from one section to the next due to meandering current and lateral deviation. Further east the isolines appear slightly wavy, but mainly horizontal till near the Ocean Weather Station METRO (2°E) where the isolines declines steeply towards east. These conditions appear very constant and stable, thus clearly seen on all single sections as well as on the mean section. This configuration may to some extent explain the apparently random and abrupt variations which have previously been noticed on the data from Weather Station METRO (Mosby 1959), because a comparatively small lateral deviation will obviously give perceptible difference in depth of the isolines. The isolines related to the deeper water masses rise towards the continental slope, probably due to deep water transport towards north. The isolines related to the upper layers decline towards east near the slope, indicating strong geostrophic currents towards north.

We may therefore conclude that the transition layer becomes more narrow towards east. The temperature gradient is twice as great in the eastern part as in the western part of the section. The salinity shows the same feature and even greater difference between the vertical gradients at the eastern and the western side of the section.

The effect of the vertical mixing will not be studied any further in this report, but only mentioned as one of the problems which should be paid attention to in future investigations.

The hydrographic features which have been dealt with above, may also be seen on the sections based on single stations although in a more obscure form.

## GENERAL DESCRIPTION OF THE CURRENT SYSTEMS IN THE NORWEGIAN SEA.

The Norwegian Sea is dominated by a system of surface currents, forming a great counterclockwise circulation (Fig. 9).

The Atlantic current enters the Norwegian Sea mainly through the Faroe-Shetland Channel, and runs in northeasterly direction following the continental slope along the coast of Norway. Further north it splits into different branches, one of which runs into the Barents Sea, another continues northward along the coast of Spitsbergen and finally enters the Polar Sea. At about  $77^{\circ}$ - $78^{\circ}$ N one branch turns westward, crossing the Norwegian Sea forming a subsurface current under the East Greenland current.

The East Greenland current originates in the Polar Sea running southwestward along the continental slope of the eastcoast of Greenland, and leaves the Norwegian Sea through the Denmark Strait. North of Iceland the East Iceland current runs southeastward, following the Iceland-Faroe ridge. One part of it crosses the ridge and runs into the Atlantic Ocean, while another part is absorbed by the Atlantic current.

Associated with the principal currents along the border of the Norwegian Sea there are two major eddies, one in the southern and one in the northern part of the Norwegian Sea. Together with numerous smaller quasistationary eddies, they cover the extensive areas where lateral mixing takes place.

Through these gyral water masses related to the East Greenland and East Iceland currents are intermittently transported to the eastern part of the Norwegian Sea where traces of these water masses may be encountered.

The Norwegian coastal current comprises water of Baltic origin, together with run off water from land. The coastal water is characterized by low salinity and temperature, the related current runs mainly northwards along the continent, forming a border between the Atlantic current and the coast.

The Norwegian Sea deep water is generally considered a homogeneous watertype where only very low current speeds are found. Recent investigations, however, show relatively great current speeds, particularly near the continental slope.

The present work does not comprise investigations on the deep water which will consequently not be dealt with any further.



## THE CURRENT CONDITIONS

The data obtained by the current meters have been corrected and applied for preliminary analysis according to the standard program at Geophysical Institute. The object of this analysis was mainly to reveal the characteristic features of the current and the temperature fields.

The current component histograms (Figs. 10 - 13) show the magnitude and the principal current conditions at the respective stations. At Station A there is an obvious instrumental failure, most likely due to a blind sector in the compass.

At Station A the current meter was located to 200 m depth and the current speed varies between 10-75 cm/sec, most frequently 25-30 cm/sec. The mean north component is 12.7 cm/sec, the mean east component -4.2 cm/sec, and the most frequent direction is 290-300° magnetic. The latter values should be regarded with care, due to the errors mentioned above.

The progressive vector diagram (Fig. 18a) indicates a northwesterly water transport during the period concerned. At buoy Station B the current meter was located at 200 m depth, and the registrations show quite unique current conditions. The speed ranges between 0-50 cm/sec, most frequently between 15-20 cm/sec. The mean north component is only 0.2 cm/sec whereas the mean east component is 10 cm/sec. Consequently, at this station there is an eastward directed flow with small or insignificant components towards north and south. This feature is also clearly seen on the progressive vector diagram which indicates a period of about one month.

Buoy Station C was anchored in the vicinity of the Ocean Weather Station METRO and the current meters were located at 200 m and 350 m depth. Unfortunately, the instrument at 350 m was lost during the launching, and the instrument at 200 m depth failed after 20 days. The registrations

obtained during the first 20 days, show relatively stable currents, mainly directed towards north. The current speed ranges from 15-80 cm/sec most frequently between 20-55 cm/sec, thus a relatively strong current towards north. Average north component is 25 cm/sec and average east component is determined to 2.4 cm/sec.

On Station D the current meter was located at 350 m. The current conditions are obviously quite stable and very similar to those on Station C.

The current speed varies between 10-60 cm/sec, most frequently between 25-30 cm/sec. The most frequent current direction is  $350-360^{\circ}$ .

Mean north component is 17.3 cm/sec and the mean east component is 0.4 cm/sec. Comparing the progressive vector diagram for Stations C and D, there is a striking similarity between the two tracks for the period concerned. The progressive vector diagram for Station D (Fig. 18a) shows a strong eastward flow during the period 21-25 April. The temperature registrations shows a drastic rise of about  $4^{\circ}$  for the same period, indicating that the instrument has been located in entirely different water masses. The temperature decreases towards west, and the rise of temperature cannot be explained by a mere lateral movement. The average vertical temperature gradient have been determined to about  $0.019^{\circ}/m$ , and the temperature increase thus corresponds to a vertical displacement of about 210 m. It can be shown that a low pressure system with corresponding strong southwesterly winds has passed the buoy station during this period. A closer examination of the current registrations shows current speeds exceeding 50 cm/sec directed towards east/northeast till about 0300 hour on April 26. About this time the current direction changes abruptly towards north/northwest. The moment for this event seems to correspond very closely with a front passage indicated on the weather-maps.

A similar temperature increase is seen on Figure 7, Station D for the period April 6-12 without the same effect on the corresponding current condition. At Station C there is no current speed registrations after April 22. However, the current direction has been recorded showing the same change in current direction as on Station D. The temperature registrations at Station C, Figure 7 shows periodical vertical displacements and does not reveal any particular rise of temperature for the period which has been dealt with above.

It is reason to believe that the phenomena which have been discussed is closely related to the propagation and passage of the weathersystem. An investigation of these conditions is considered to be of great importance, but beyond the intention of this report.

The progressive vectordiagram (Fig. 18a) shows that the average watertransport ranges from 10-26 cm/sec. The maximal average speed which was found at buoy Station C may not be considered relevant, because this speed is based on a shorter period of observation when strong currents were recorded on all buoy stations.

Harmonic analysis with respect to diurnal and semi-diurnal tidal periods has been applied to the current components. The analysis has been performed stepwise, applying 72 consecutive hourly observations for each step.

Current ellipses have been determined for the diurnal and semidiurnal components. Histograms, showing the most frequent length of the long axes and the most frequent orientation is given in Figure 18b.

Based on the analysis indicated above the tidal current contribution may briefly be characterized as follows:

Length of long axes

St.	Diurnal		Semidiurnal	
	Max. cm/sec	Most frequent cm/sec	Max. cm/sec	Most frequent cm/sec
A	24	12-15	24	3-6
B	21	3-6	27	0-3
C	36	6-9	36	3-6
D	30	9-12	24	9-12

On Stations A, B and C the diurnal contributions are greater than the semidiurnal. At Station D, however, the semidiurnal is more frequently the greater. It can be shown that the ratio between the short and the long axes is generally rather small, thus giving "flat" ellipses. The orientation of the long axes is, for all stations, concentrated around  $180^\circ$ . The tidal current will therefore give contribution mainly in the east/west direction. At Stations A and B the current is found to rotate both ways with no dominating direction. On Stations C and D, however, the current is most frequently rotating clockwise.

The present analysis should be regarded as preliminary results which has been made in order to indicate the magnitude and the main characteristics of the tidal contribution. A more sophisticated analysis will be performed at Woods Hole Oceanographic Institution, comprising power spectrum and harmonic analysis with respect to the tidal constituents.

## GEOSTROPHIC CURRENT

The meridional geostrophic current across the section is illustrated by Figures 19-23. The reference level is the pressure surface at 1000 m depth, except at the eastern end of the section approaching the continental shelf, where it is the pressure surface at 600 m depth.

Figures 19 and 20 show the mean conditions and it is clear that there are three major zones of north-going flow and one minor zone, whilst there are four zones of south-going flow. The mean speed of the north-going flow is maximal in the middle of the section, between Stations 9 and 10, where it reaches  $15 \text{ cm/sec}^{-1}$  near the surface. It reaches  $11 \text{ cm/sec}^{-1}$  in a zone at the eastern end of the section, between Stations 1 and 3, and  $8 \text{ cm/sec}^{-1}$  towards the western end, between Stations 14 and 15. The mean speeds of the south-going flow are much less and are maximal at  $7 \text{ cm/sec}^{-1}$  at the western end of the section, between Stations 19 and 20 and in a zone towards the eastern end, between Stations 6 and 7. The streakiness of the geostrophic flow reflects the waviness of the isotherms and isohalines in the mean temperature and salinity distributions given in Figures 3 and 4.

The changes in the geostrophic current with time are shown in Figures 21-23 and the outstanding feature of these three figures is the permanence of the alternating bands of north and south-going current. Further, it can be seen that the instantaneous flow can reach speeds which are twice those of the mean flow. At the surface there are three clearly defined bands of permanent north-going flow which do not change their positions greatly during the entire period of the survey.

- (I) at the eastern end of the section between  $4^{\circ}$  and  $6^{\circ}$ E; varying in width between 20 and 40 n.miles; speeds up to  $30 \text{ cm/sec}^{-1}$  and more
- (II) in the centre of the section between  $1^{\circ}$  and  $3^{\circ}30'E$ ; varying in width between 10 and 40 n.miles; speeds up to  $30 \text{ cm/sec}^{-1}$  and more
- (III) towards the western end of the section between  $1^{\circ}W$  and  $2^{\circ}E$ ; varying in width between 20 and 60 n.miles; speeds up to  $20 \text{ cm/sec}^{-1}$  and more.

Between these are similar permanent bands of south-going flow with similar widths and velocities. Thus, changes from a  $30 \text{ cm/sec}^{-1}$  north-going flow to a  $30 \text{ cm/sec}^{-1}$  south-going flow can occur within a distance of 15 n.miles, for example, between Stations 6 and 8 on 14 April.

There are also bands of flow which are less permanent features. For instance, after 27 April an extra band of south-going flow and an extra band of north-going flow appear at the eastern end of the section. Similarly, extra bands appear in the middle of the section at the beginning of April.

At 200 m depth the pattern of flow is somewhat less complex, but the main features are similar to those found at the surface. The speeds are less than those at the surface. Only that part of the section which is in the vicinity of Station D is included in the 350 m diagram (Fig. 23), but it repeats the features of the 200 m diagram and shows a further reduction in speed with increasing depth.

## GEOSTROPHIC MASS TRANSPORT

The distribution of the potential energy anomaly along the section (Fofonoff 1962) against time for the period of the survey is given in Figure 24a. The spacing of the isopleths allows the magnitude of the north-going and south-going mass transport to be seen at any point at any time. This transport is that between the surface and 1000 m depth, except at the eastern end of the section where it is that between the surface and 600 m depth. The alternating bands of north and south-going flow seen in the geostrophic current analysis are, of course, readily apparent. The heaviest mass transport to the north occurs close to the continental shelf between  $5^{\circ}$  and  $6^{\circ}$ E and in the middle of the section between  $2^{\circ}30'$  and  $3^{\circ}30'$ E. The latter flow is flanked on its eastern side by the heaviest south-going transport. The mean mass transport of Atlantic water, (defined as water with a salinity greater than 35 ‰), between successive pairs of stations along the section for the period of the survey is shown in Figure 24b. It has the same features as the geostrophic current pattern and the mass transport. The mean total transport of Atlantic water amounts to  $1.55 \times 10^6$  tonnes/sec<sup>-1</sup> northwards, whereas the mean total mass transport as defined above amounts to  $1.08 \times 10^6$  tonnes/sec<sup>-1</sup> northwards. Thus there is a mean total transport southwards of  $0.47 \times 10^6$  tonnes/sec<sup>-1</sup> below the Atlantic water.

## DISCUSSION

The geostrophic currents shown in Figures 19-23 can be compared with the observed currents shown in Figures 14-18a. Figure 22 indicates clearly that the geostrophic current in the vicinity of Station A changes direction in the same way as the observed current at 200 m depth at Station A given in Figure 14. The observed current is predominantly north-going as is the geostrophic flow. There are two periods with a south-going component in the observed flow, 15-20 April and 12-16 May, and these are the only two periods of south-going geostrophic flow.

Comparison of Figures 15 and 22 shows that at Station B a north-going component at 200 m depth changes to a south-going one on 6 April in both the observed and geostrophic flows but, whereas the observed current reverses again on 8 April and stays with a north-going component until 12 April, the geostrophic flow remains south-going until 29 April, apart from a short period of reversal on 15-20 April. The observed flow is south-going from 12 April until 24 April when the north-going component reappears and remains uninterrupted until 17 May; on the other hand, the geostrophic flow seems to remain north-going after 29 April apart from a short period between 6 and 10 May. These disagreements between the observed and geostrophic flows are very probably due to nothing more than the way in which the isopleths were drawn in Figure 22; the analyst who prepared this figure was not allowed to see Figure 15. It is easy to adjust the isopleths to bring the direction of geostrophic flow into agreement with that of the observed.

Figure 16 shows that the observed current at 200 m depth at Station C was north-going from 5 to 22 April, except during 8 and 9 April. This is in agreement with Figure 22.



However, Figure 17 shows the observed current at 350 m at Station D had a north-going component over all the period 6 April-18 May, whilst Figure 23 shows the geostrophic flow to have been largely south-going. Part of this disagreement could again be due to the way in which Figure 23 is drawn, but not all of it, as is shown by the fact that a south-going geostrophic flow occurs in the mean distributions between Stations 12 and 13, which straddle Station D (Figs. 19 and 20).

From Figure 18a it is possible to obtain the mean speed of the north-going component over the whole period during which a current meter was working and to compare this with the mean speed of the geostrophic flow given in Figure 19. Such a comparison gives the following results:-

Station	Mean Speed	Mean Speed
	Observed N-going component (cm/sec <sup>-1</sup> )	Geostrophic N-going component (cm/sec <sup>-1</sup> )
A (200 m)	13	8
B (200 m)	0	0
D (350 m)	18	-1

Station C cannot be considered in this way because the current meter did not function for the whole period of the survey. This comparison brings out the striking disagreement between the observed and geostrophic flow at Station D. The method is not completely valid, however, because the current meter were working continuously whereas the geostrophic mean values are based on 17 discrete observations. A better method might be to compare the current meter observations at the actual times of the 17 crossings, as given in Figures 14-17 with the geostrophic values obtained then. However, it proves difficult to decide which is the correct speed of the geostrophic current because of the way in which Figures 22 and 23 have to be drawn. In the first place, these figures are based on the values of the mean geostrophic current over successive 10 n. miles.

intervals and these are plotted at the midpoints of successive pairs of stations, so that a certain amount of smoothing is introduced. In the second place, the drawing of the isopleths depends on the judgement of the analyst. Thus, the values of the speed of the geostrophic current derived from Figures 22 and 23 are not completely reliable, particularly in areas where steep gradients occur. Station A is in such an area, and in addition suffers from the disadvantage that it is close to the point where the reference level changes. The difficulty of drawing isopleths in the region of Station B has already been mentioned. If we consider Stations C and D where the difficulties are less, then we find that at Station C, at 200 m depth for the six crossings which were made before the current meter stopped functioning, the mean difference between the observed north-going component and the geostrophic current, amounts to 11 cm/sec<sup>-1</sup>, with the observed values the higher (south-going components being regarded as negative). The maximal difference was found on crossing No. 5 when the observed value was 49 cm/sec<sup>-1</sup> and the geostrophic 20 cm/sec<sup>-1</sup>. At Station D, at 350 m depth for the 16 crossings that were made before the current meter was recovered, the mean difference is 16 cm/sec<sup>-1</sup> with the observed values the higher: the greatest difference was on crossing No. 8 when the observed value was 34 cm/sec<sup>-1</sup> and the geostrophic -4 cm/sec<sup>-1</sup>. It is of interest to note that at both stations there is a tendency for the highest difference to occur during the two periods of low temperature recorded by the two meters and shown in Figure 7.

During crossings Nos. 2 and 4, R.V. "Ernest Holt" used GEK: the north-going current component so obtained is shown in Figure 21. A multiplier of 34.5 to convert millivolts to cm/sec<sup>-1</sup> was used following the work of Vaux (1965) at Andenes. No agreement can be seen between this component and the geostrophic current. In fact, if

the sign of the GEK record was reversed it would agree much better. This lack of agreement between the GEK signal and the geostrophic current is surprising in view of the good agreement found by Lee (1962) at  $74^{\circ}25'N$  latitude in the continuation of the current which we are examining here.

## VERTICAL OSCILLATIONS

It has been mentioned above that the depth of the isolines vary greatly with respect to space and time. The short periodic variations are presumably eliminated by the process of 25 hours running mean, a process which reduces the amplitudes of the long periodic variations as well. In a similar way the process of averaging reduces the vertical variations of the isolines in the mean sections. Provided the oscillations are due to progressive waves or travelling whirls, the effect will vanish in the mean sections due to the same process of averaging.

Standard deviation for the depth of the isotherms has therefore been determined in order to indicate the relative magnitude of the vertical displacements or amplitudes (Fig. 6). Average temperature has been determined by applying the method of 25 hours running mean on the temperature recordings from the current meters (Fig. 7). A more comparable parameter is the standard deviation of the temperature divided by the vertical temperature gradient.

It may thus be shown that the maximum amplitudes are normally located at 200-300 m depth, which corresponds with the middle depth of the Atlantic water. Further down the vertical displacement seems to decrease towards bottom. Figure 6 indicates that the magnitude of the amplitudes increases eastwards towards the coast. This feature is confirmed by the registrations on the buoy stations.

The investigations dealt with comprises only observations taken along a vertical section, and it is therefore impossible to tell anything about propagation speed or direction. Neither is it possible to state whether the oscillations are due to internal waves or whirls. Sælen (1959) concludes that whirls are the most probable explanation. Internal waves which have been reflected from the coast may also cause similar configurations.

Observations on short periodic variations with respect to time were carried out at position 11 in the vicinity of buoy Station C. Hydrographic stations were taken at hourly intervals; from May 20 at 1500 hours to May 21 at 1800 hours, thus covering a period of 27 hours.

The isotherms are plotted versus time in Figure 26; indicating oscillations where the periods are about 6 hours. The greatest amplitudes appear at 200 m and at 700 m depths. This is in agreement with fact that the greatest standard deviation for the depth of the isotherms is generally found at 200 m depth. The layer between 200 and 700 m seems subjected to only very small vertical oscillations.

Periods of 6 hours are frequently found in the Norwegian Sea. (Helland-Hansen and Nansen 1909).

## FINAL REMARKS

In the preceding chapters of this report we have shown how our knowledge of the physical oceanography of the Norwegian Sea has been extended by the 1967 study of variability. It is clear that there are various problems which require further investigation. For example, we need to see whether the pattern of alternating bands of north- and south-going flows is repeated at other seasons and at the same season in other years; to investigate the mechanisms responsible for this pattern and the effect of various weather systems upon it and upon the temperature and salinity distributions; and to study the reasons for the difference between the observed flow and the geostrophic in the middle of the section. The further analysis of the data collected will without doubt yield even more knowledge and further problems, and in this connexion we think that the power spectrum and harmonic analysis might yield information about the tidal and inertial currents and that detailed statistical analysis might throw more light on the correlations between the fluctuations in various parameters.

However, it is already clear from the analysis so far that further experiments in the Norwegian Sea in the region of the  $66^{\circ}\text{N}$  parallel would be a fruitful line of research. We feel that such investigations should be three dimensional so as to take into account the variability in the north-south direction as well as the east-west, and that the period of observation should be longer than 2 months. There is an obvious need for more buoy stations than were used in 1967, and the number of depths sampled by recording instruments at each station should be increased. Such a programme would not call for a large number of research ships: one or two in the area at the

same time over the whole period of the survey would be sufficient. These vessels should keep the buoy stations under surveillance and should make temperature and salinity observations, preferably with temperature-salinity-depth recording systems, and studies of the weather development in conjunction with the weather ship at Ocean Weather Station METRO. There is probably a need to study the Lagrangian form of the motion as well as the Eulerian. This could be done by using neutrally-buoyant (Swallow) floats. Such a programme would need to be organized on an international basis, but we think that its execution would not call for more than three participating countries from Europe. We hope that the International Council for the Exploration of the Sea will give this proposal due consideration at its 1968 meeting.

## REFERENCES

- AANDERAA, I. 1964. A recording and telemetering instrument. Tech. Rep. NATO Subcomm. Oceanogr. Res., (16).
- FOFONOFF, N.P. 1962. Machine computations of mass transport in the North Pacific Ocean. J. Fish. Res. Bd. Can., 19, 1121-41
- HELLAND-HANSEN, B. 1934. The Sognefjord Section: Oceanographic Observations in the northernmost part of the North Sea and the southern part of the Norwegian Sea. James Johnstone Memorial Volume 257-474. Univ. Press Liverpool. 348 pp.
- HELLAND-HANSEN, B. and NANSEN, F. 1909: The Norwegian Sea. Rep. Norw. Fish. Mar. Inv. Vol. II. 1909, No.2. Oslo.
- LEE, A. 1962. The effect of the wind on water movements in the Norwegian and Greenland Seas. Mitt. Inst. Meeresk., Univ. Hamb., (1) 353-73.
- MOSBY, H. 1959. Deep water in the Norwegian Sea. Geof. Publ. Vol. XXI, No. 3. Oslo.
- SÆLEN, O.H. 1959. Studies in the Norwegian Atlantic Current. Part I: The Sognefjord Section. Geof. Publ. 20 (13). 28 pp.
- SÆLEN, O.H. 1963. Studies in the Norwegian Atlantic Current. Part II: Investigations during the years 1954-59 in an area west of Stad. Geof. Publ. 23 (6) 82 pp.
- VAUX, D 1965. Current measuring by towed electrodes; observations in the Arctic and North Sea, 1953-59 Fishery Invest., Lond., Ser. 2. 23, (8).



TABLE I  
Hydrographic Sections.

<u>No.</u>	<u>Ship</u>	<u>Dates</u>
1	"Ernest Holt"	4-7 April
2	" "	7-9 April
3	" "	9-11 April
4	" "	12-14 April
5	"Helland-Hansen"	17-19 April
6	" "	19-22 April
7	" "	22-24 April
8	"Ernest Holt"	29 April-2 May
9	" "	2-4 May
10	" "	4-5 May
11	" "	5-7 May
12	"Helland-Hansen"	10-11 May
13	" "	11-12 May
14	" "	13-14 May
15	" "	14-15 May
16	" "	16-17 May
17	" "	17-18 May

TABLE II

"Polarfront I"			"Polarfront II"		
<u>Date</u>	<u>Station Number</u>	<u>Station Type</u>	<u>Date</u>	<u>Station Number</u>	<u>Station Type</u>
1/4	1033	1	3/4	249	2
18/4	1034	2	4/4	250	3
19/4	1035	3	6/4	251	1
22/4	1036	1	7/4	252	3
24/4	1038	2	8/4	253	3
27/4	1039	3	10/4	254	2
Total 6 stations			11/4	255	3
<u>Observation depths (meters)</u>			12/4	256	3
			13/4	257	1
<u>Station Type 1</u>	<u>Station Type 2</u>	<u>Station Type 3</u>	14/4	258	3
0	0	0	2/5	259	3
10	10	50	3/5	260	1
25	25	150	5/5	261	3
50	50	300	6/5	262	3
75	75	400	8/5	263	2
100	100	600	9/5	264	3
150	150	1000	10/5	265	3
200			11/5	266	1
300			17/5	267	3
400			13/5	268	3
500			16/5	269	3
600			18/5	270	1
800			Total 22 stations		
1000					
1200					
1500					
1800					
Bottom					

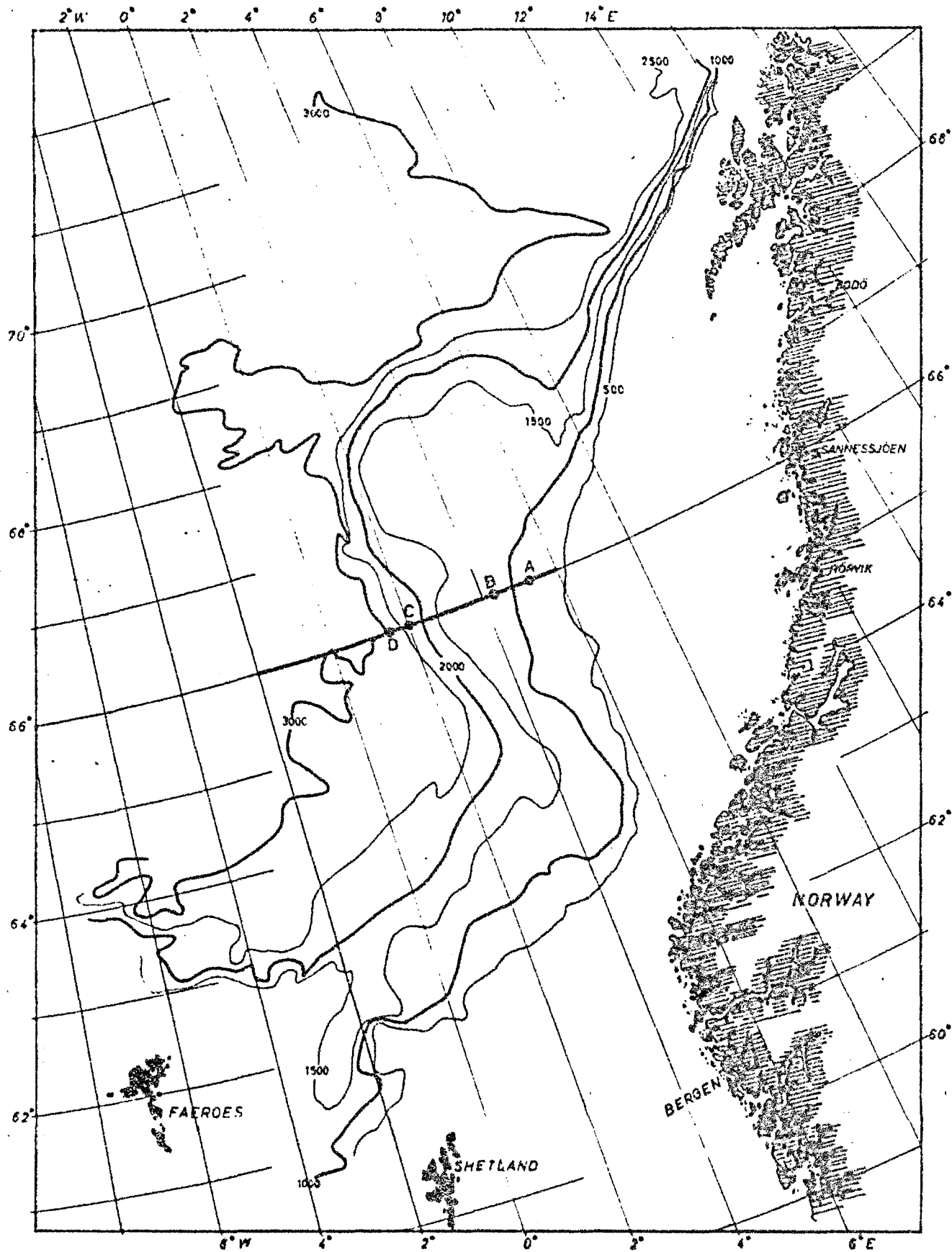


Fig. 1. Bathymetric chart of the southern part of the Norwegian Sea showing position of 66°N Section, buoystation and Ocean Weather Station METRO.

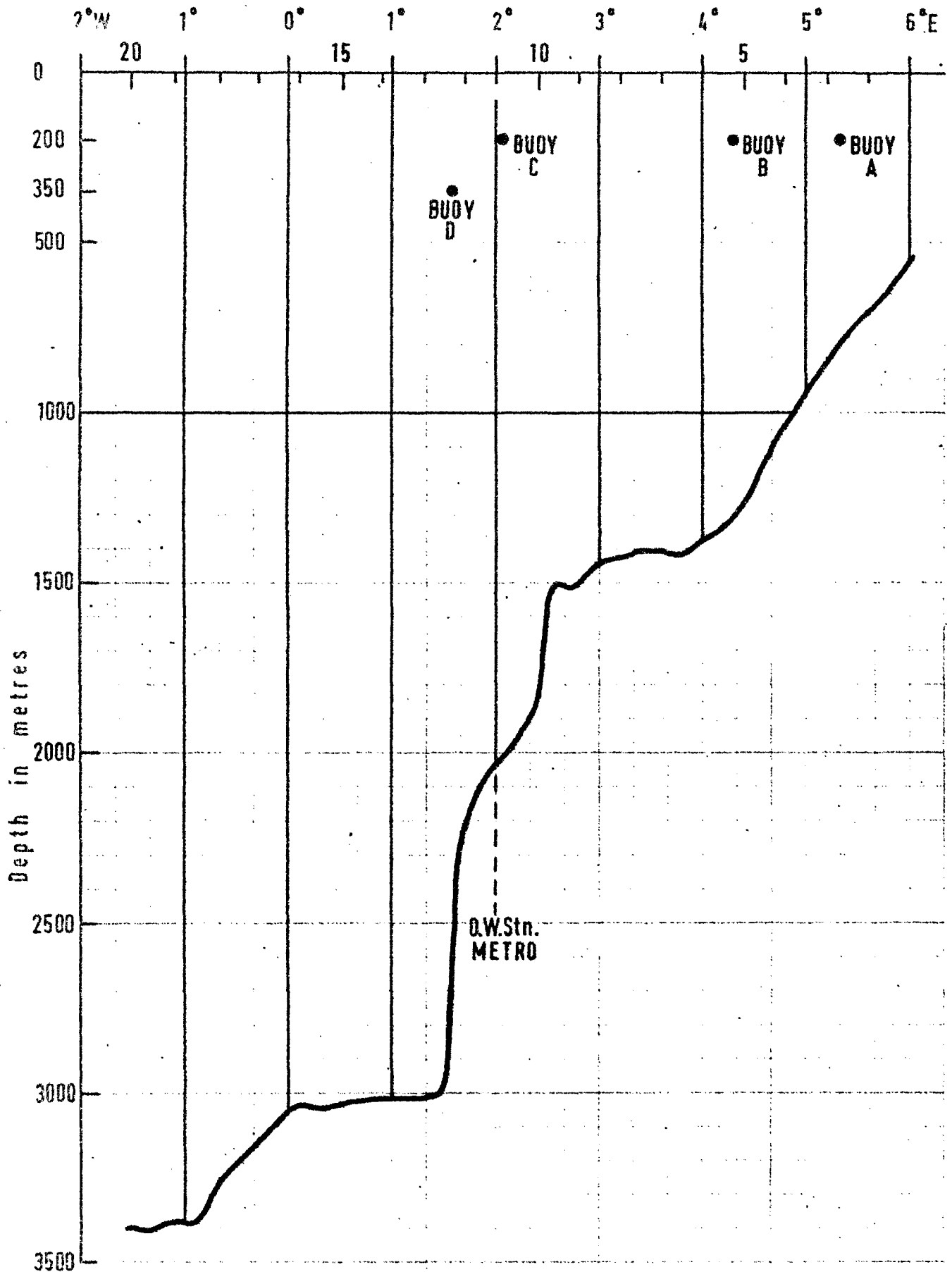
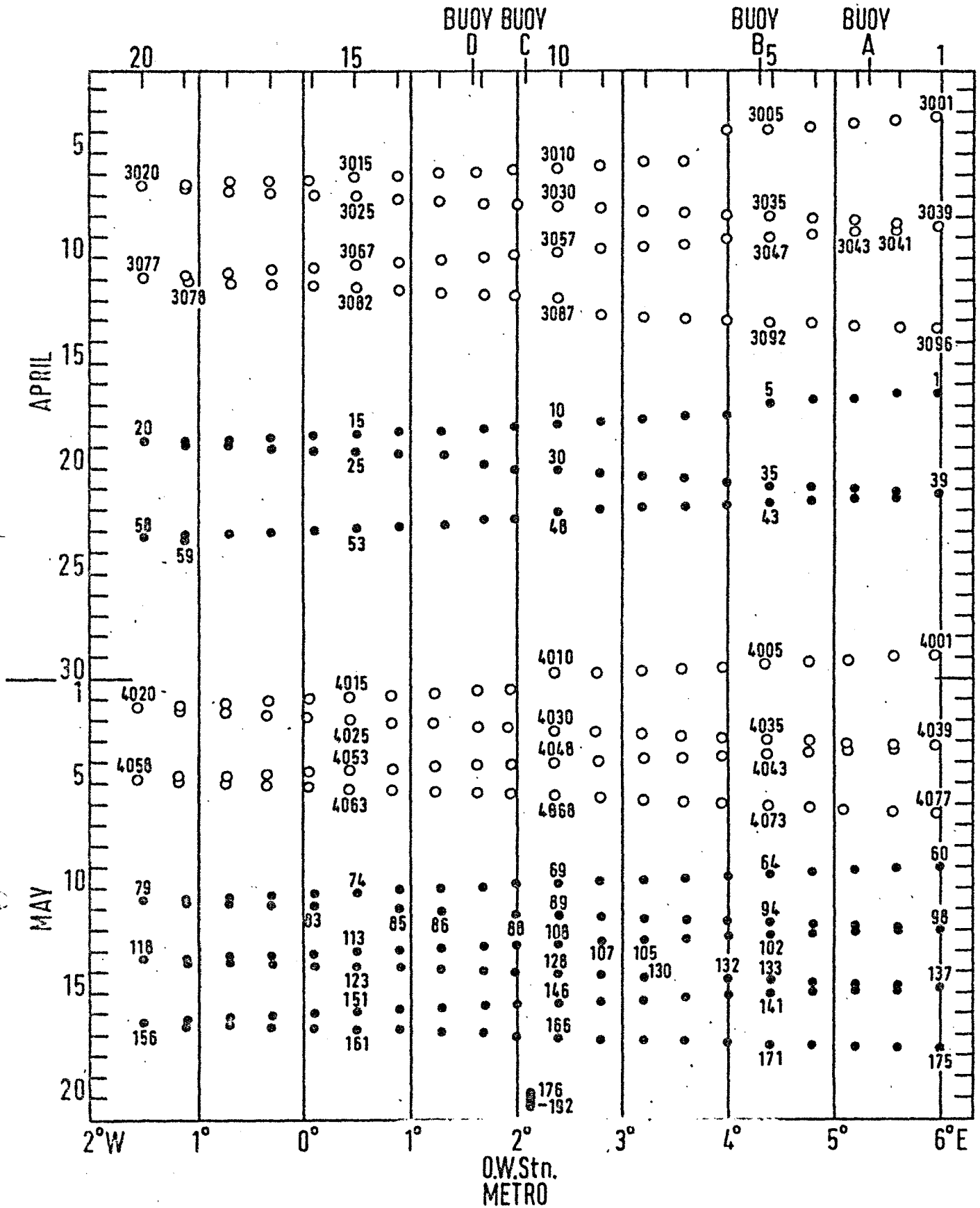


Fig. 2: Topographical section, showing the buystation, the section and Weather Station METRO.



R.V. ERNEST HOLT    ○ serial stations  
 R.V. HELLAND-HANSEN    ● serial stations

Fig 2(b): Programme of hydrographic stations worked during the period 2 April-21 May.

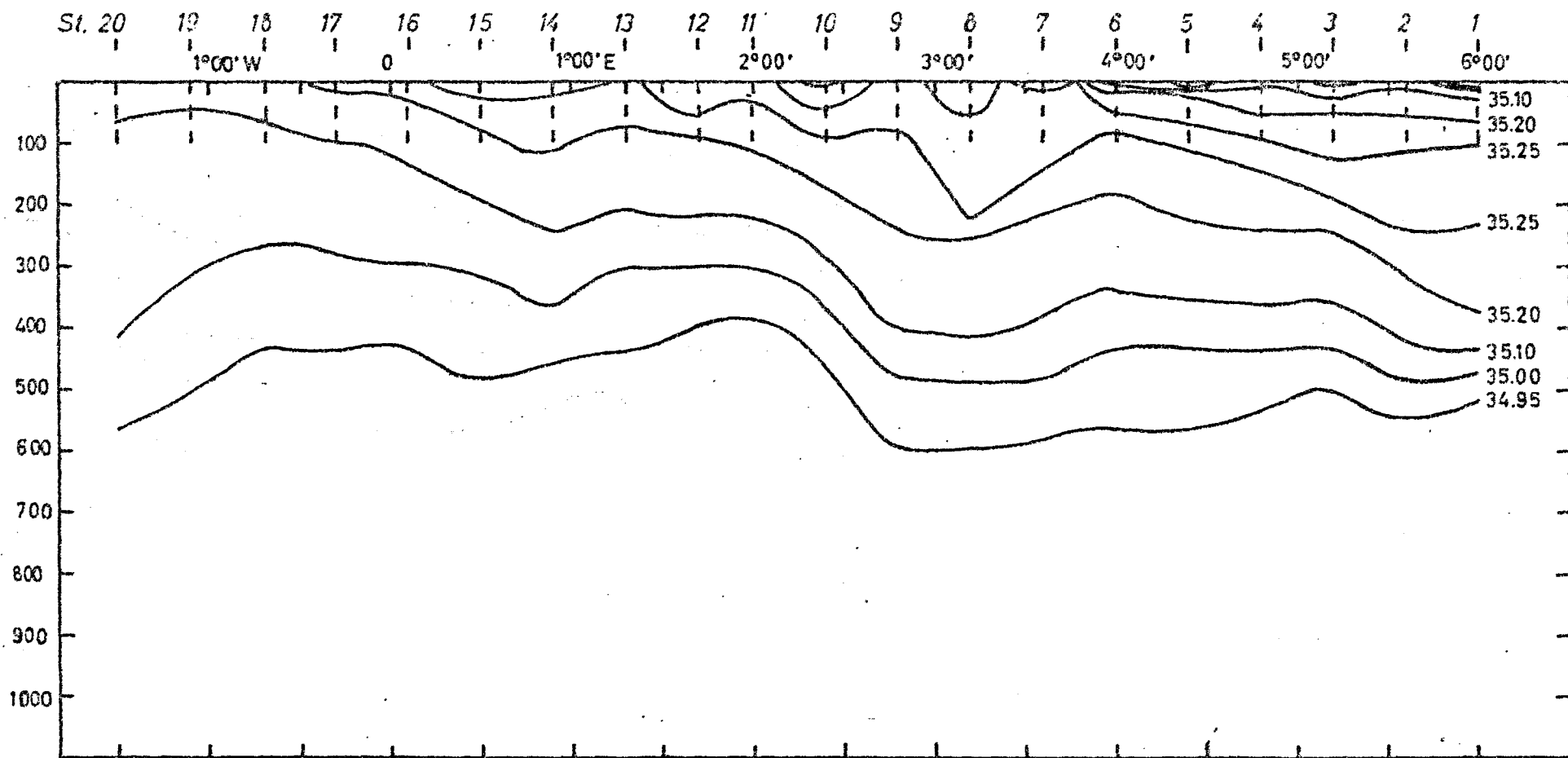


Fig. 3: 66°N: Mean salinity: Section, April 4 -  
 May 18 1967.

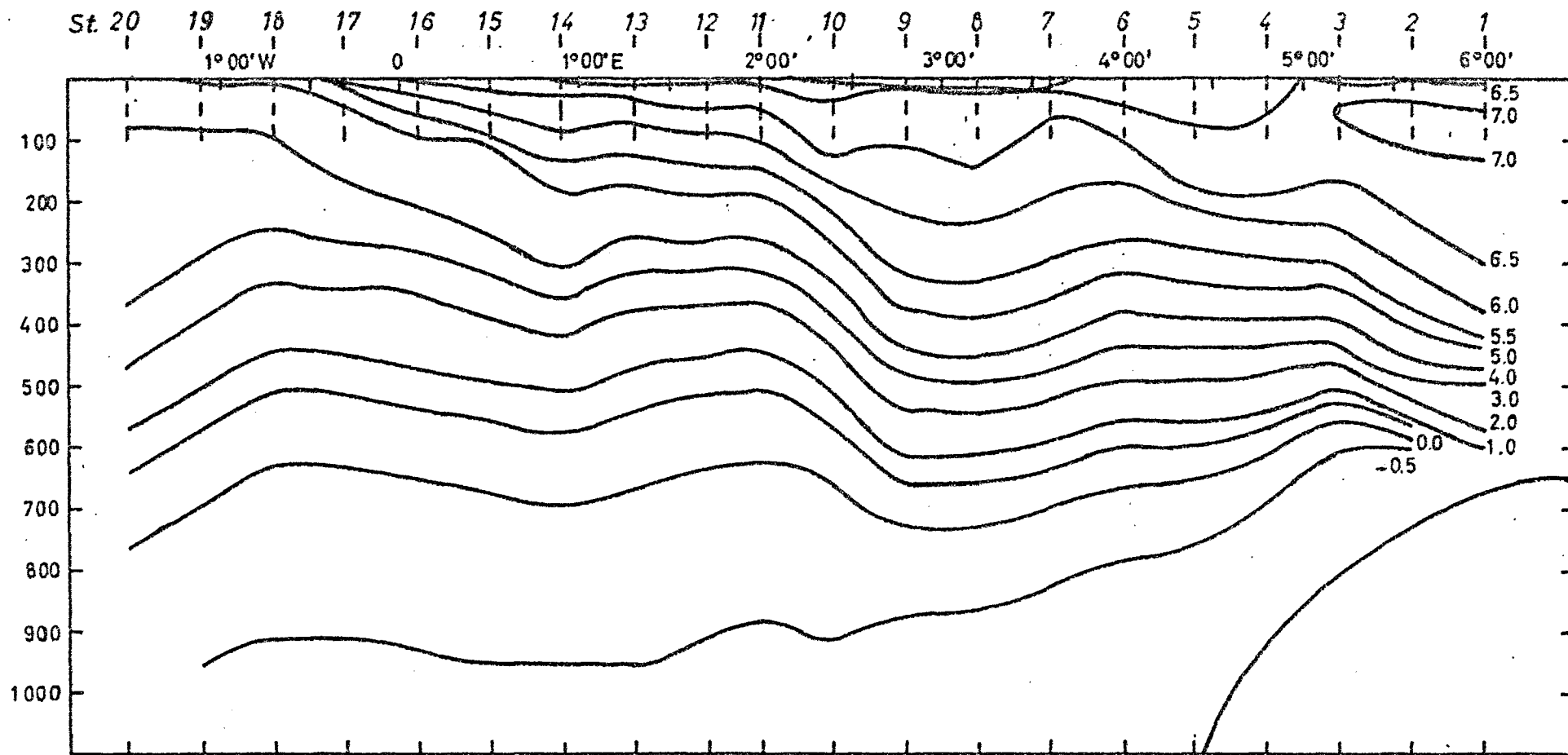


Fig. 4: 66°N: Mean temperature: Section April 4 -  
May 18 1967.

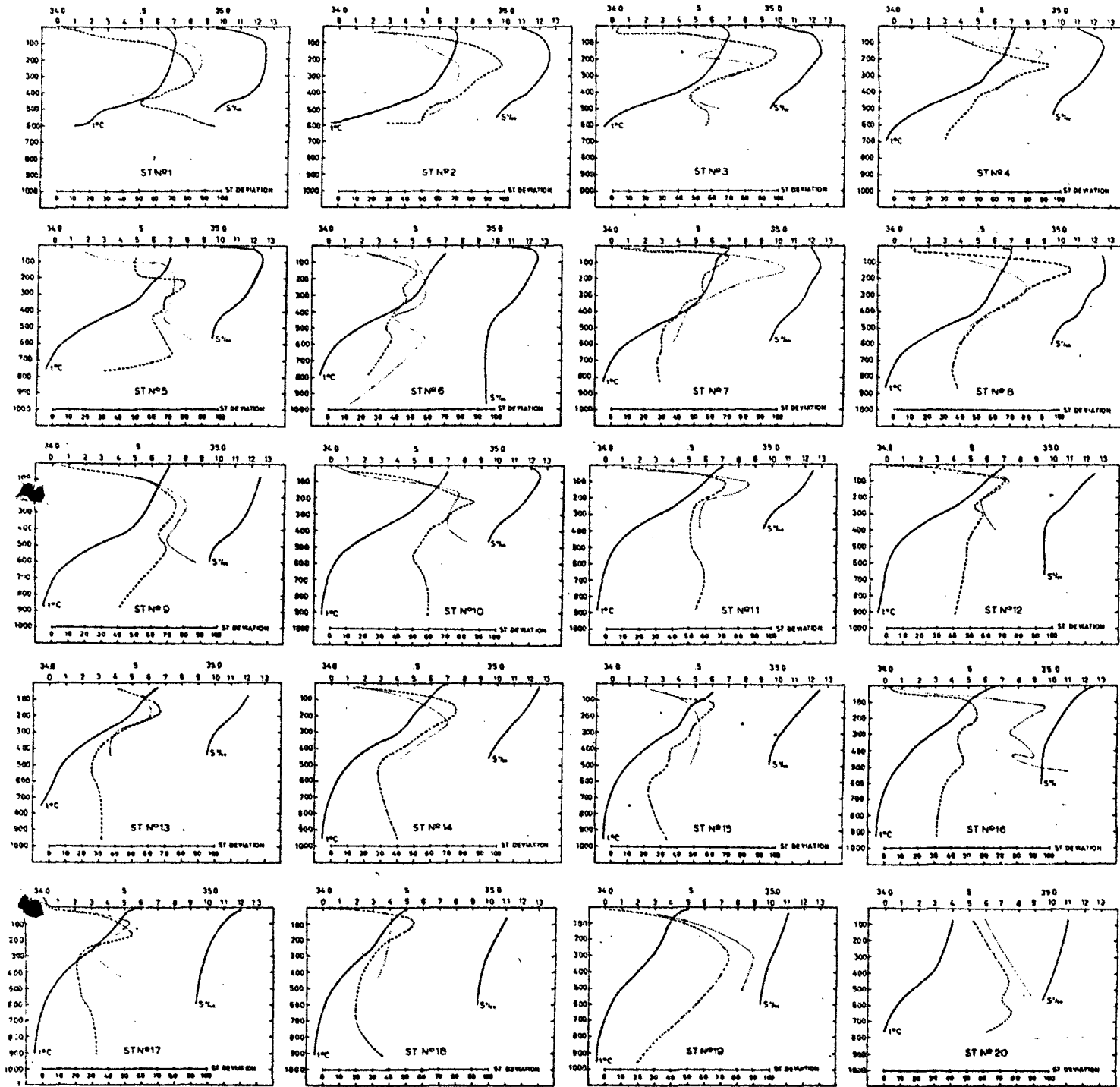


Fig. 5: Positions 1-20. Mean temperature and salinity profiles together with standard deviation. April 4 - May 18 1967.

..... Salinity standard deviation.

----- Temperature standard deviation.



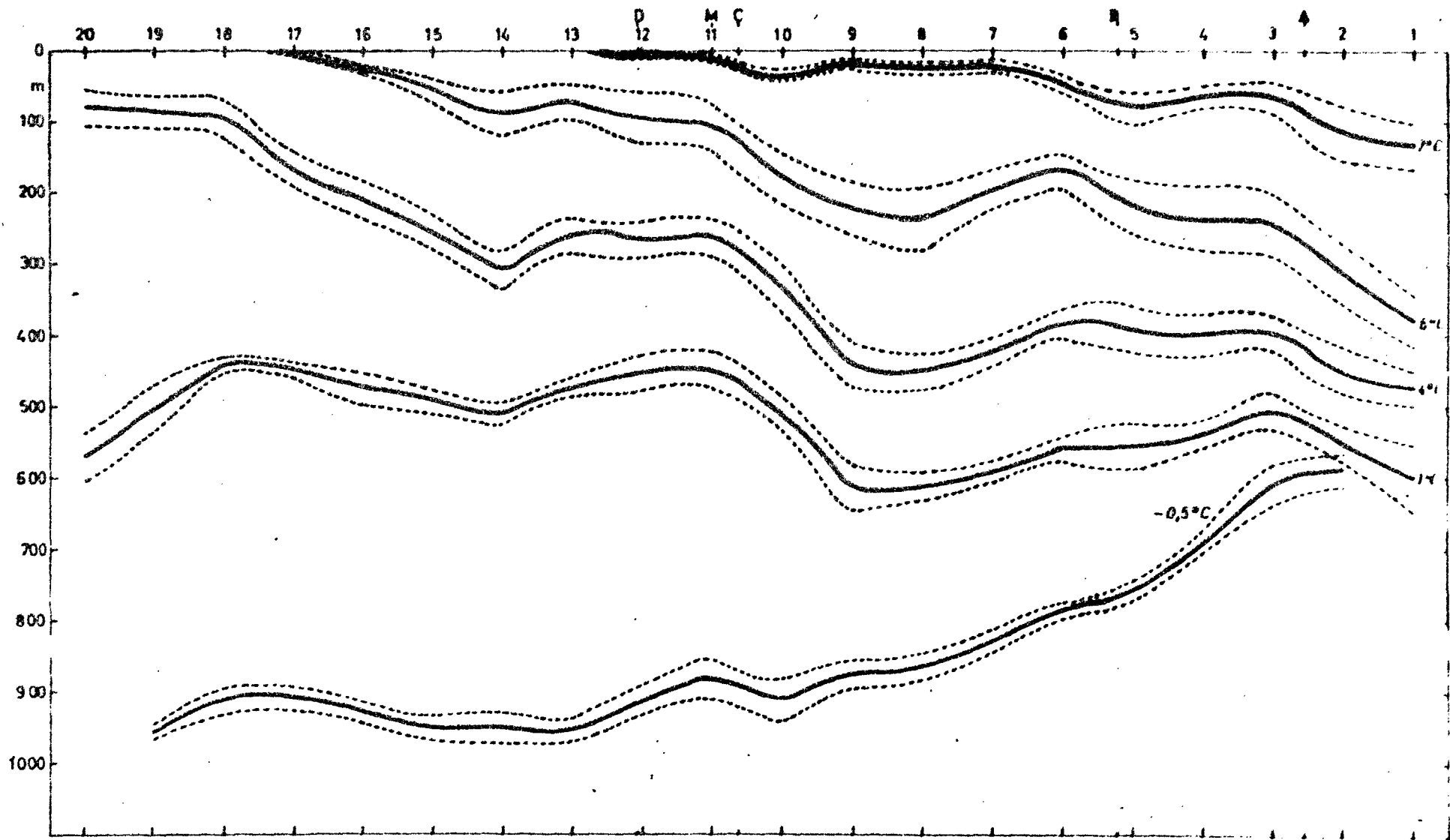


Fig. 6: 66°N: Section: Standard deviation of the depth of the isotherms: April 4 - May 18 1967.

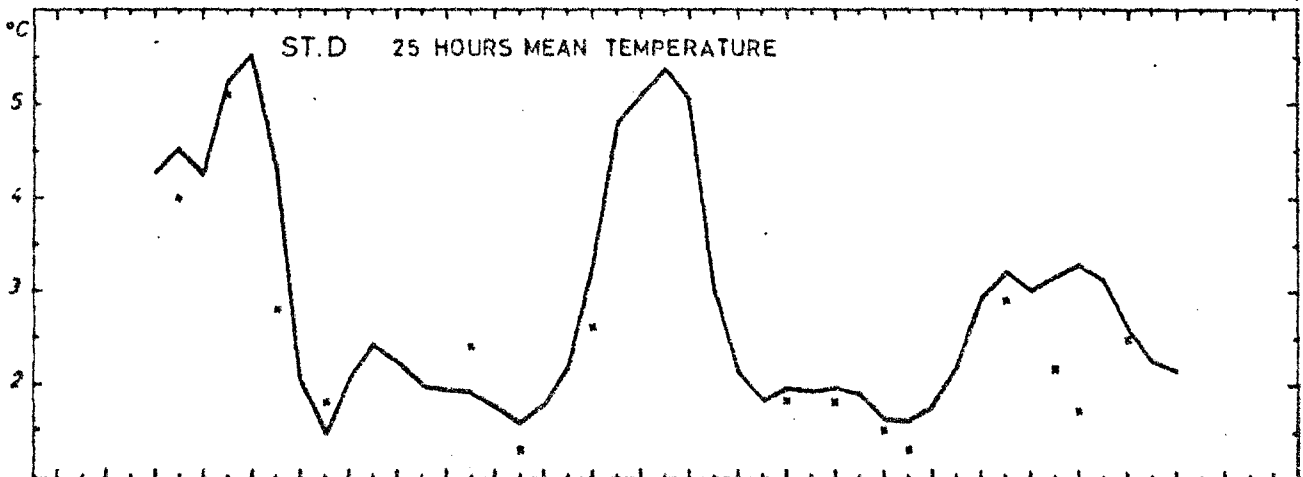
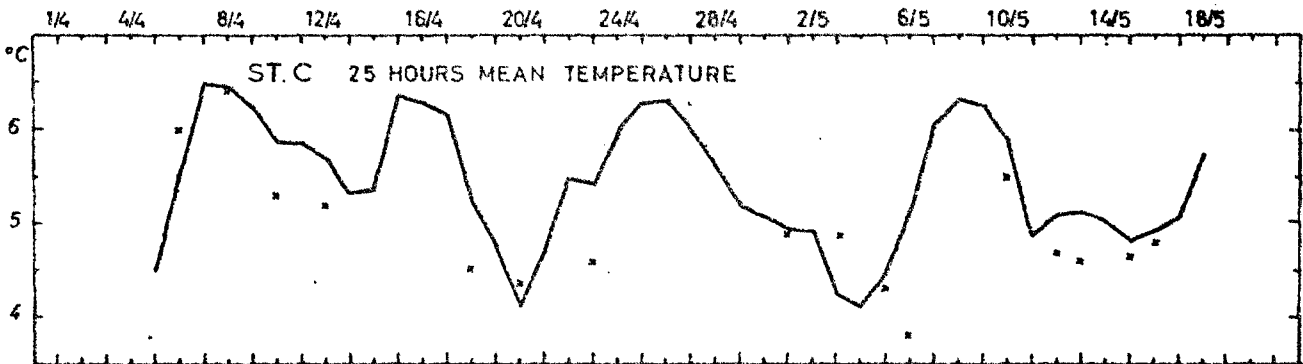
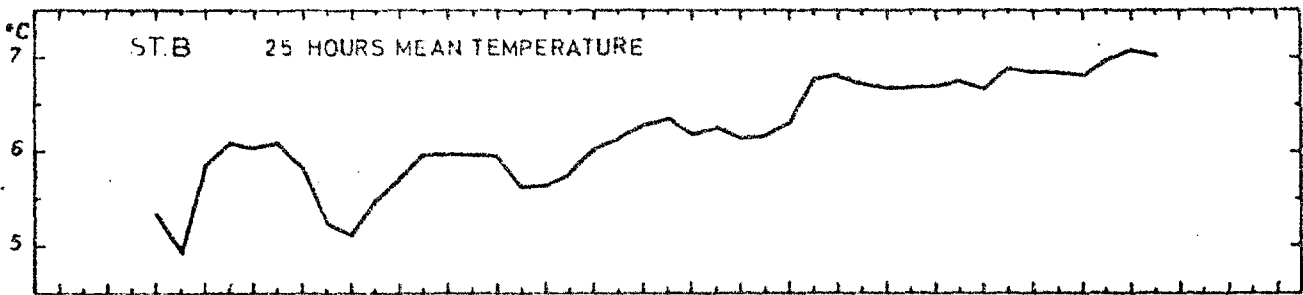
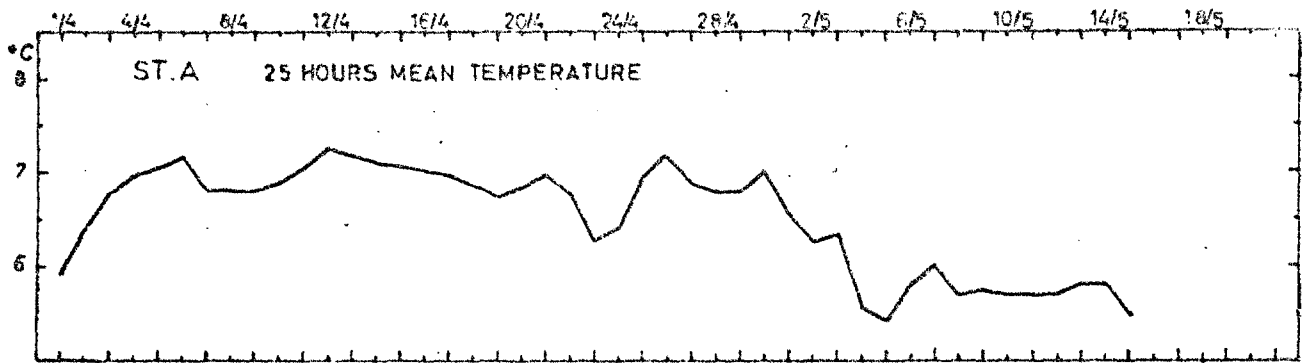


Fig. 7: Daily mean temperature: Buoystation A, B; C  
200 m: Buoystation D 350 m.

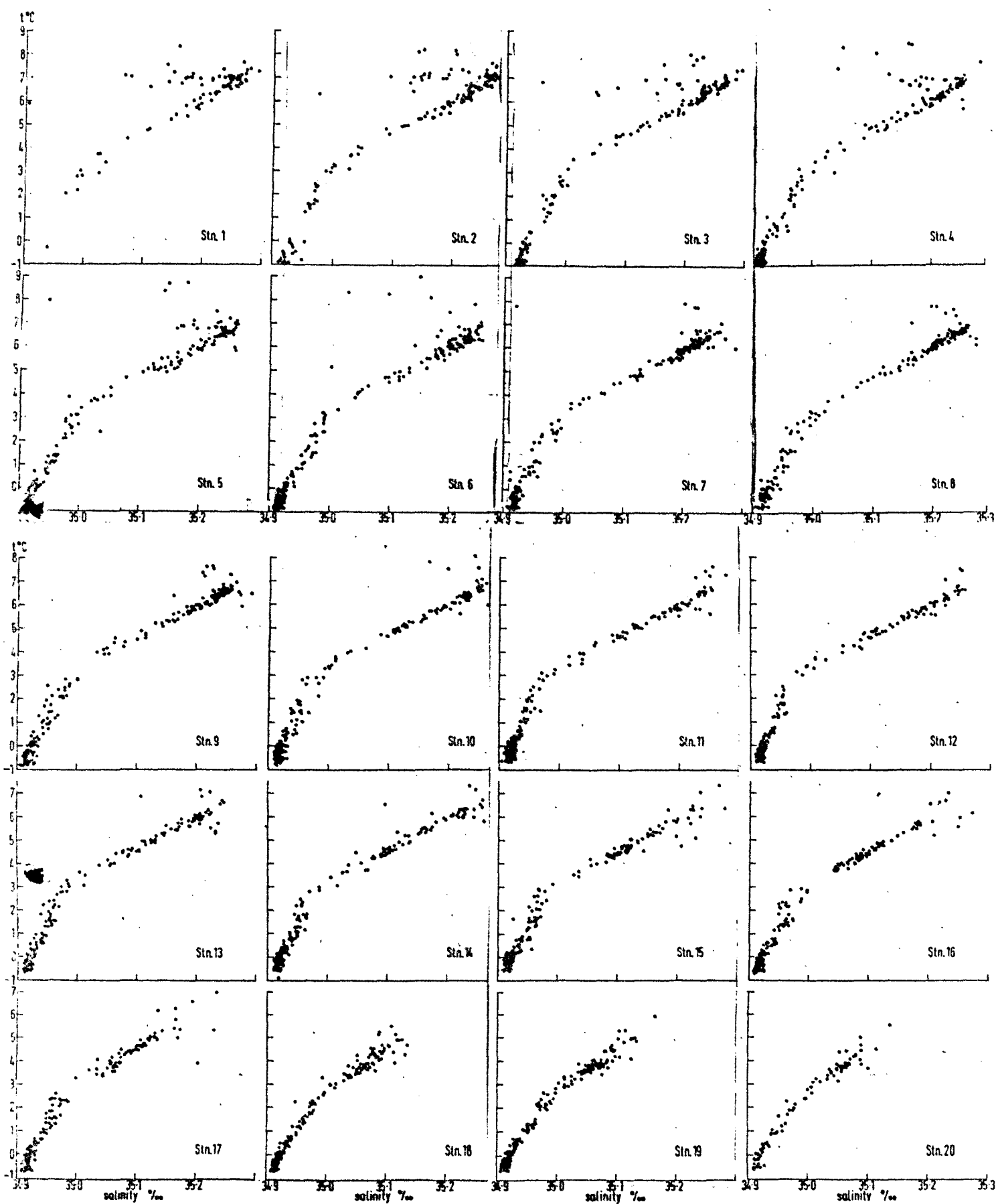


Fig. 8: T - S diagrams for stations 1-20: all workings of each station are included.

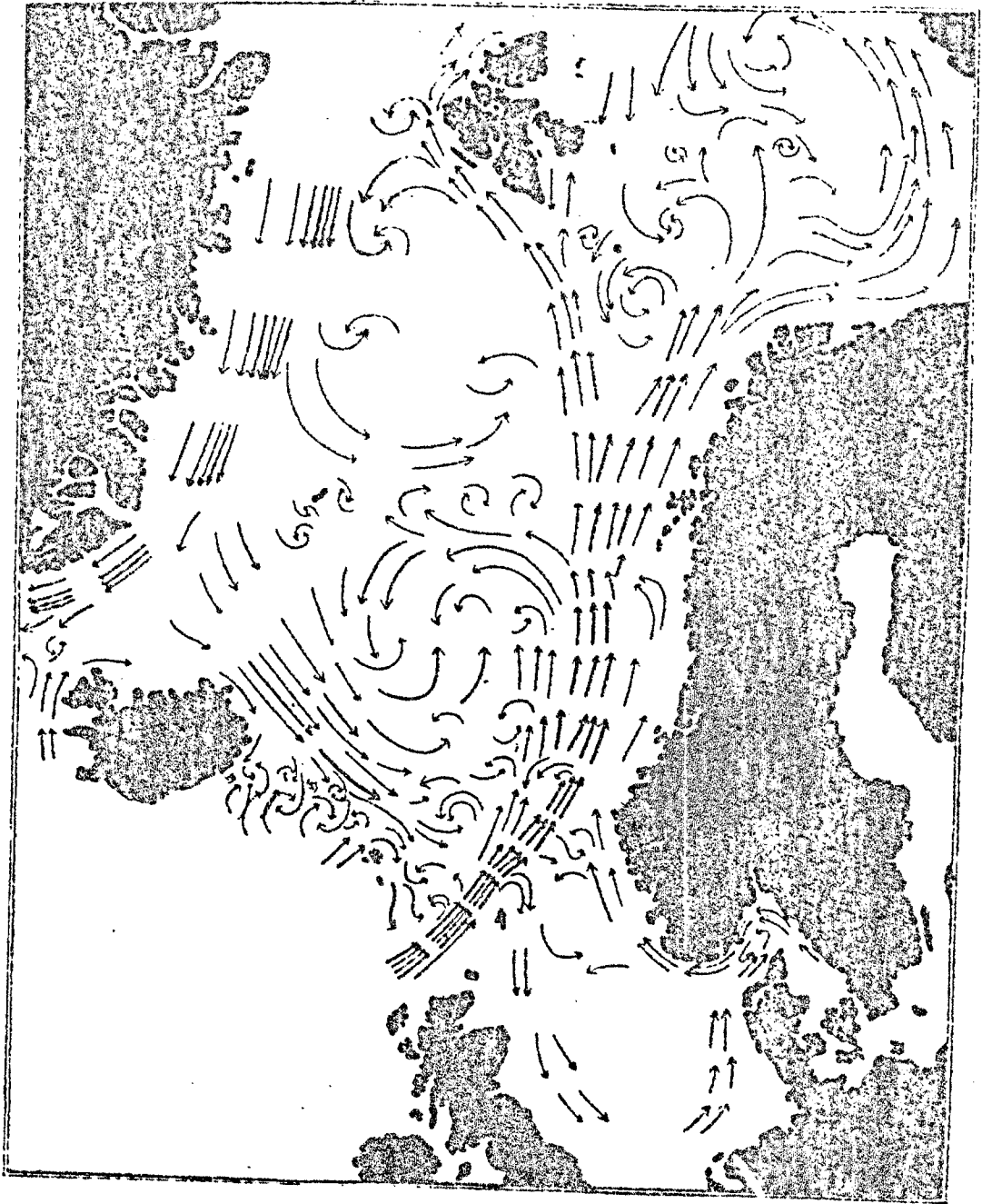


Fig. 9: General surface circulation in the southern part of the Norwegian Sea.

Helland-Hansen, B. and Nansen, F. 1909.

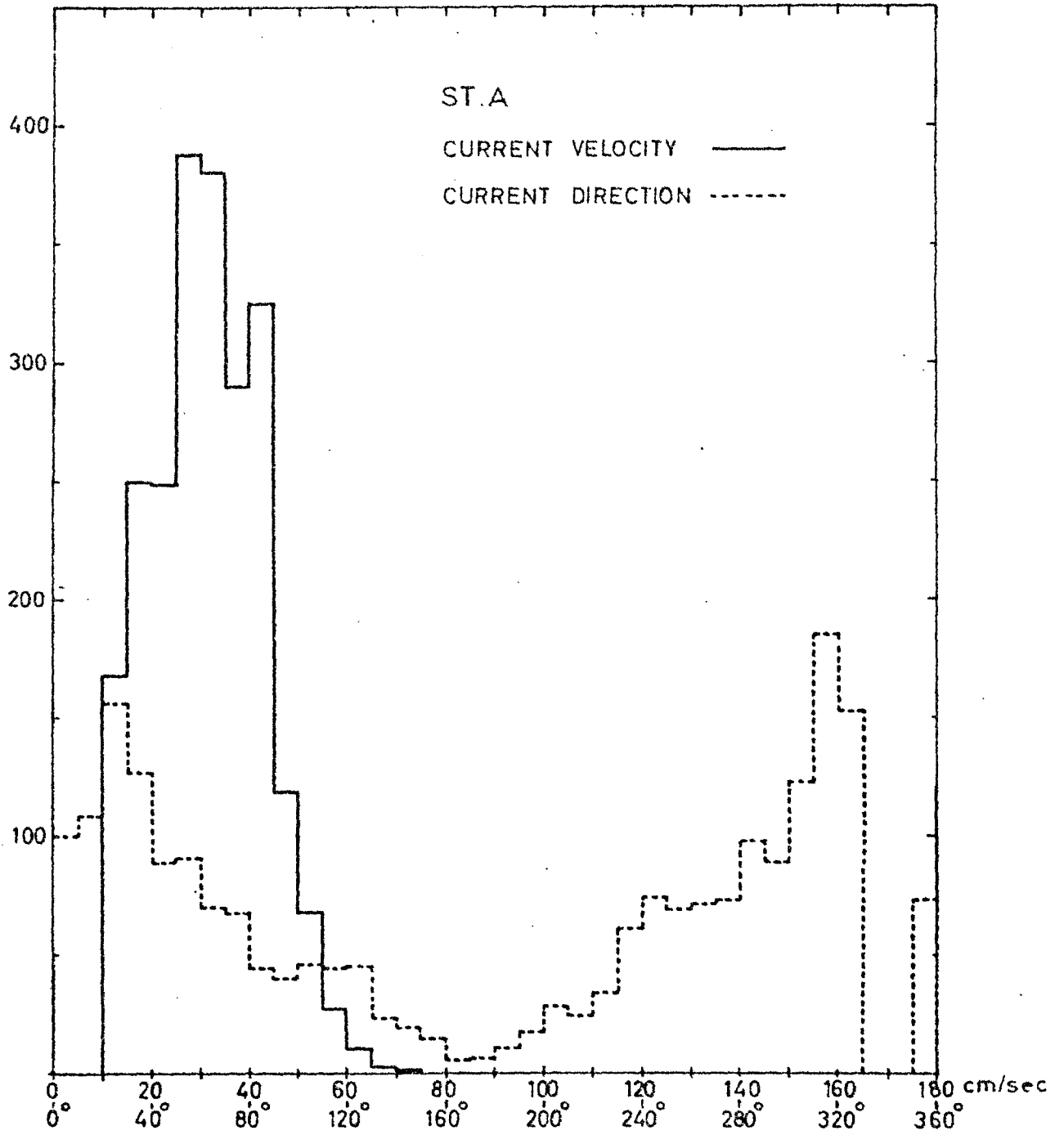


Fig. 10: Buoystation A. Histogram of current speed and direction.

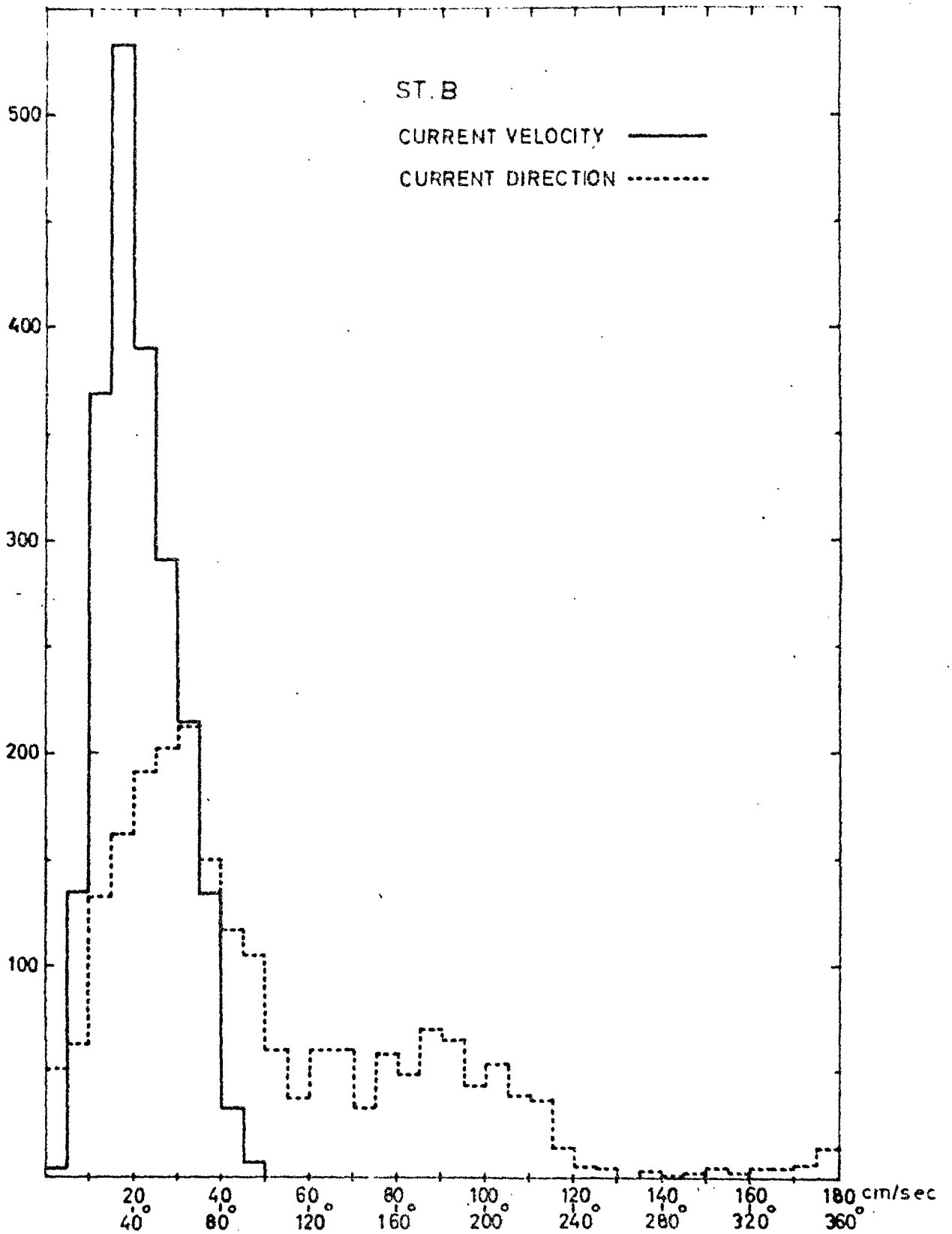


Fig. 11: Buoystation B. Histogram of current speed and direction.

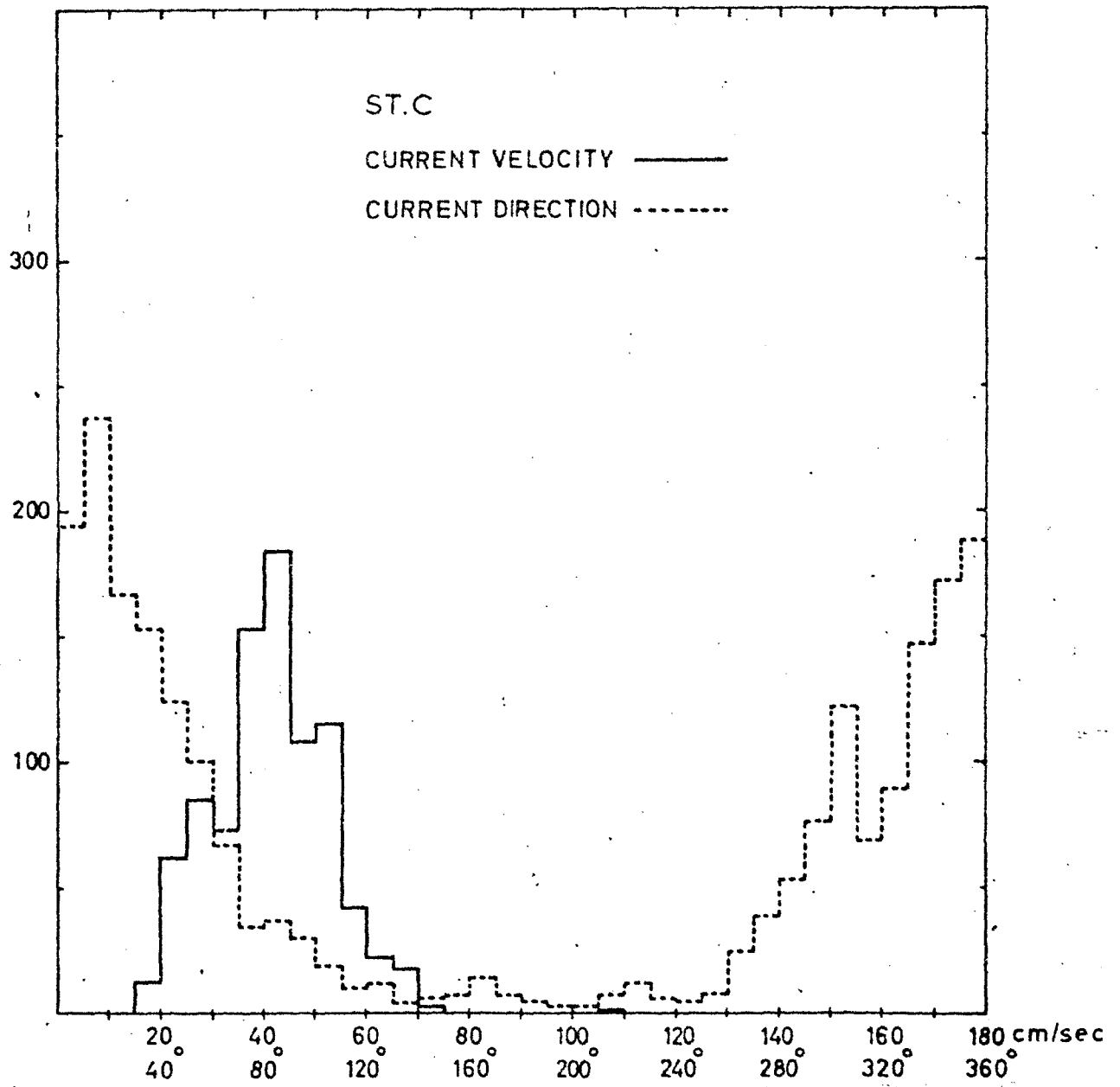


Fig. 12: Buoystation C. Histogram of current speed and direction.

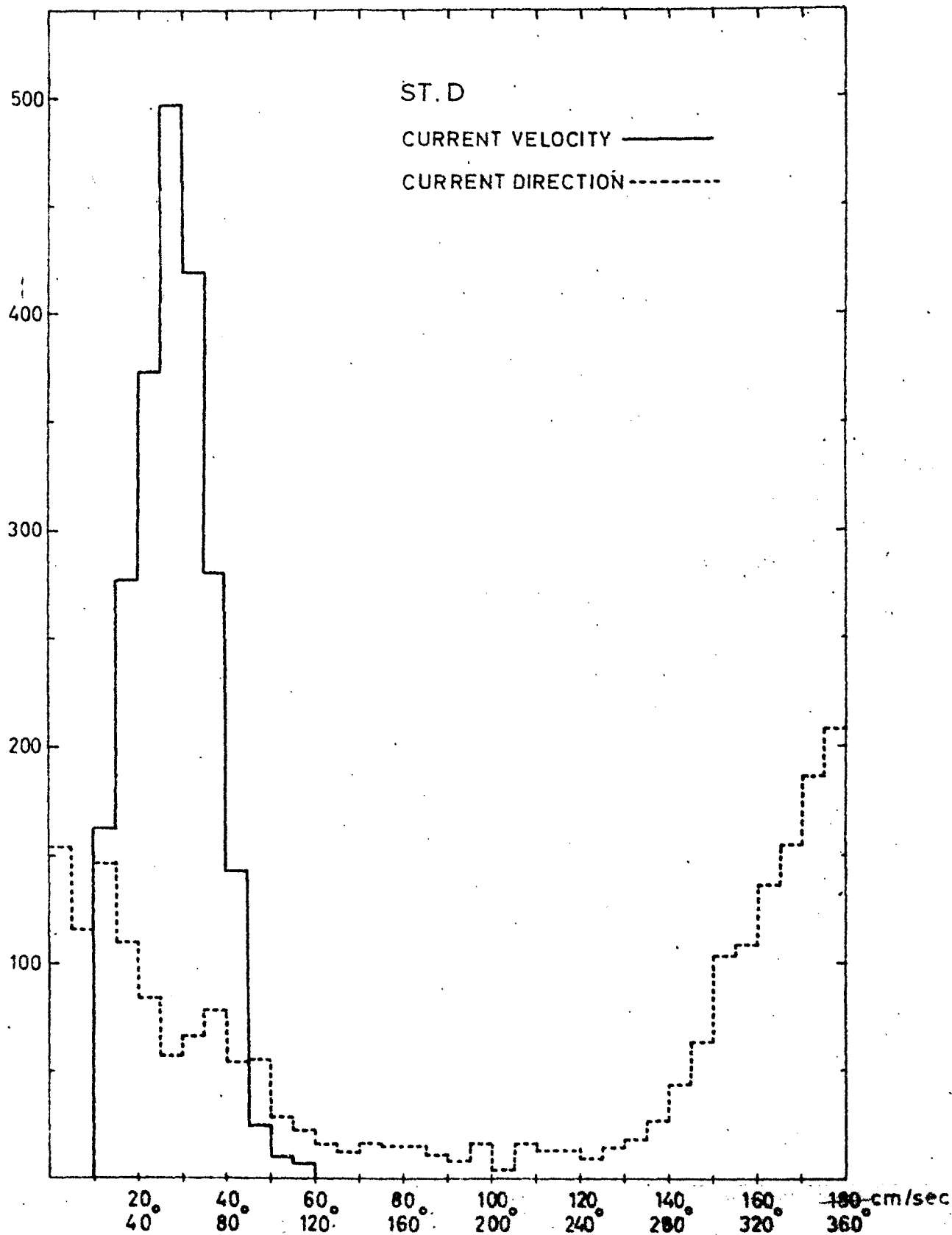


Fig. 13: Buoystation D. Histogram of current speed and direction.



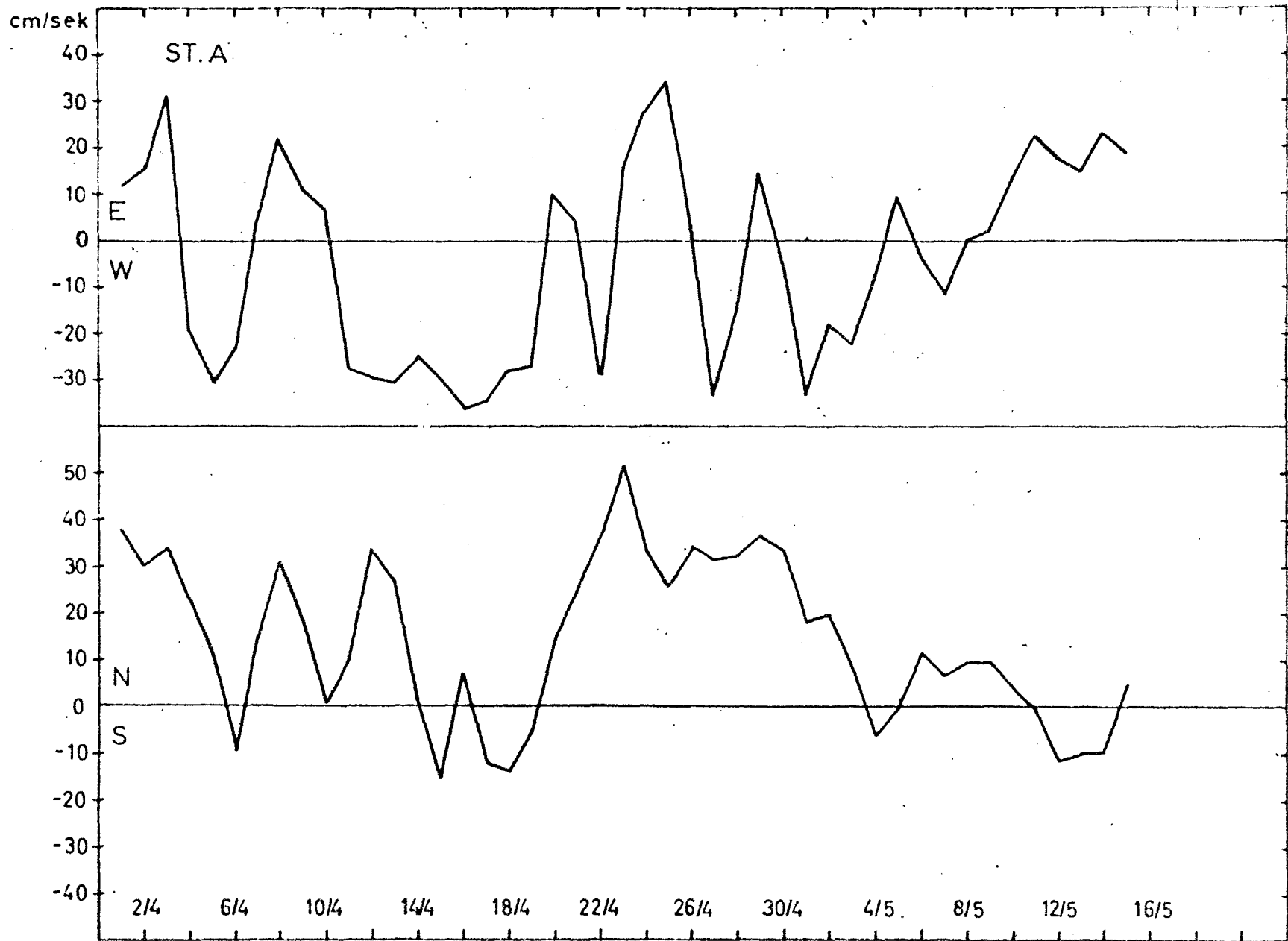


Fig. 14: Buoystation A. Daily mean current components.  
 April 4 - May 13 1967.

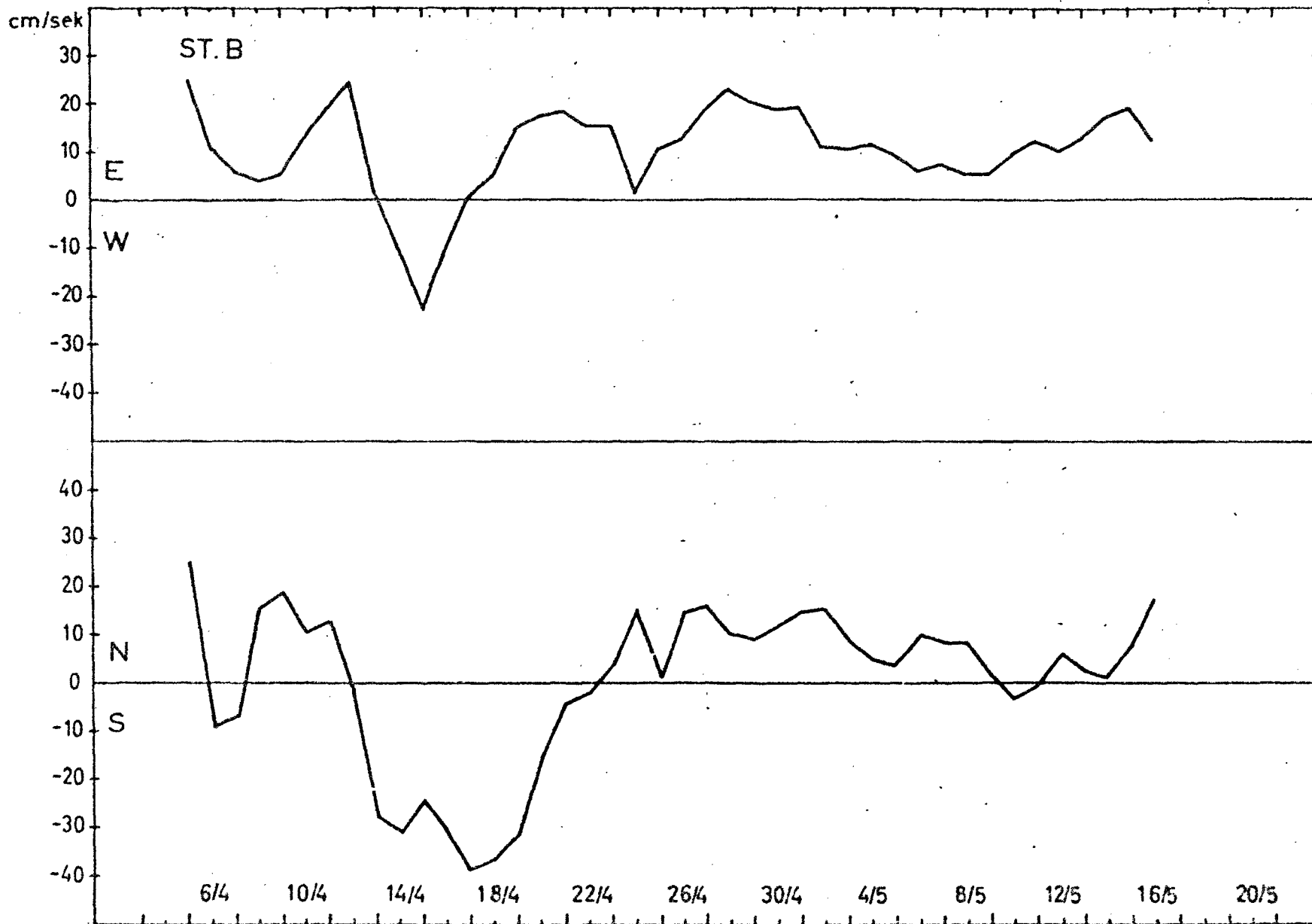


Fig. 15: Buoystation E. Daily mean current components.  
Apr. 14 - May 18 1967.

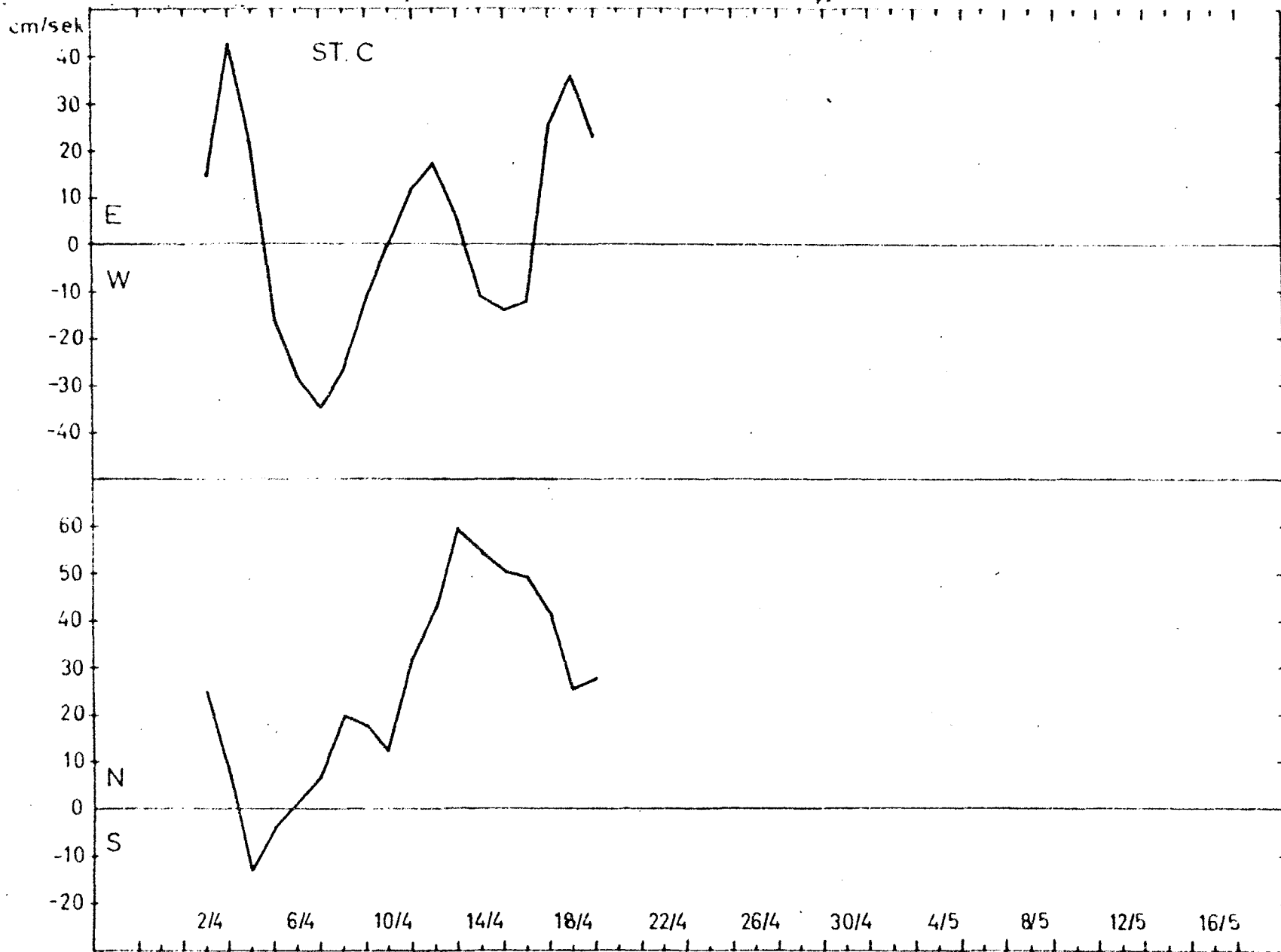


Fig. 16: Buoystation C. Daily mean current components.

April 4 - May 18 1967.

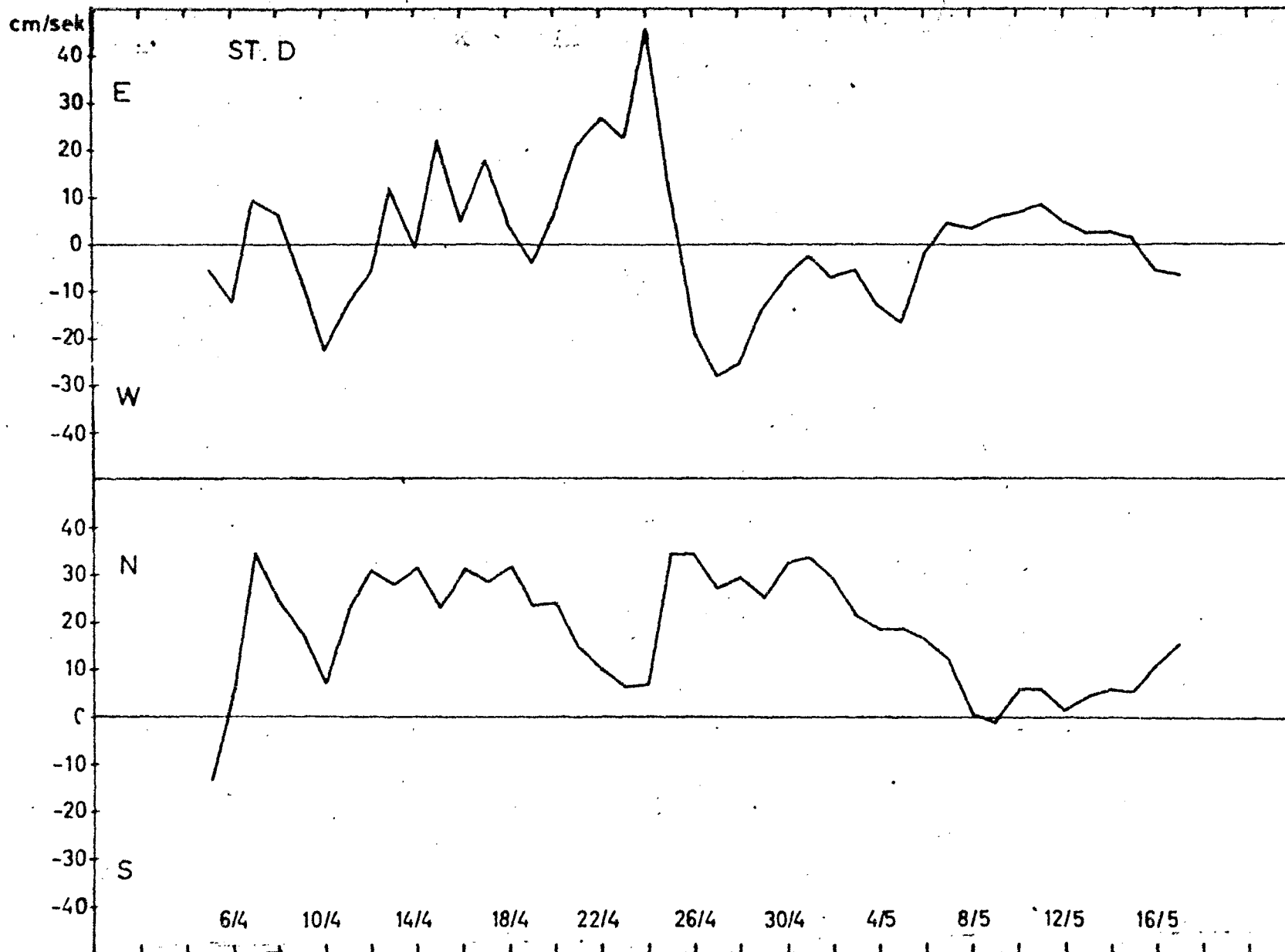


Fig. 17: Buoy Station D. Daily mean current components.

April 4 - May 18 1967.

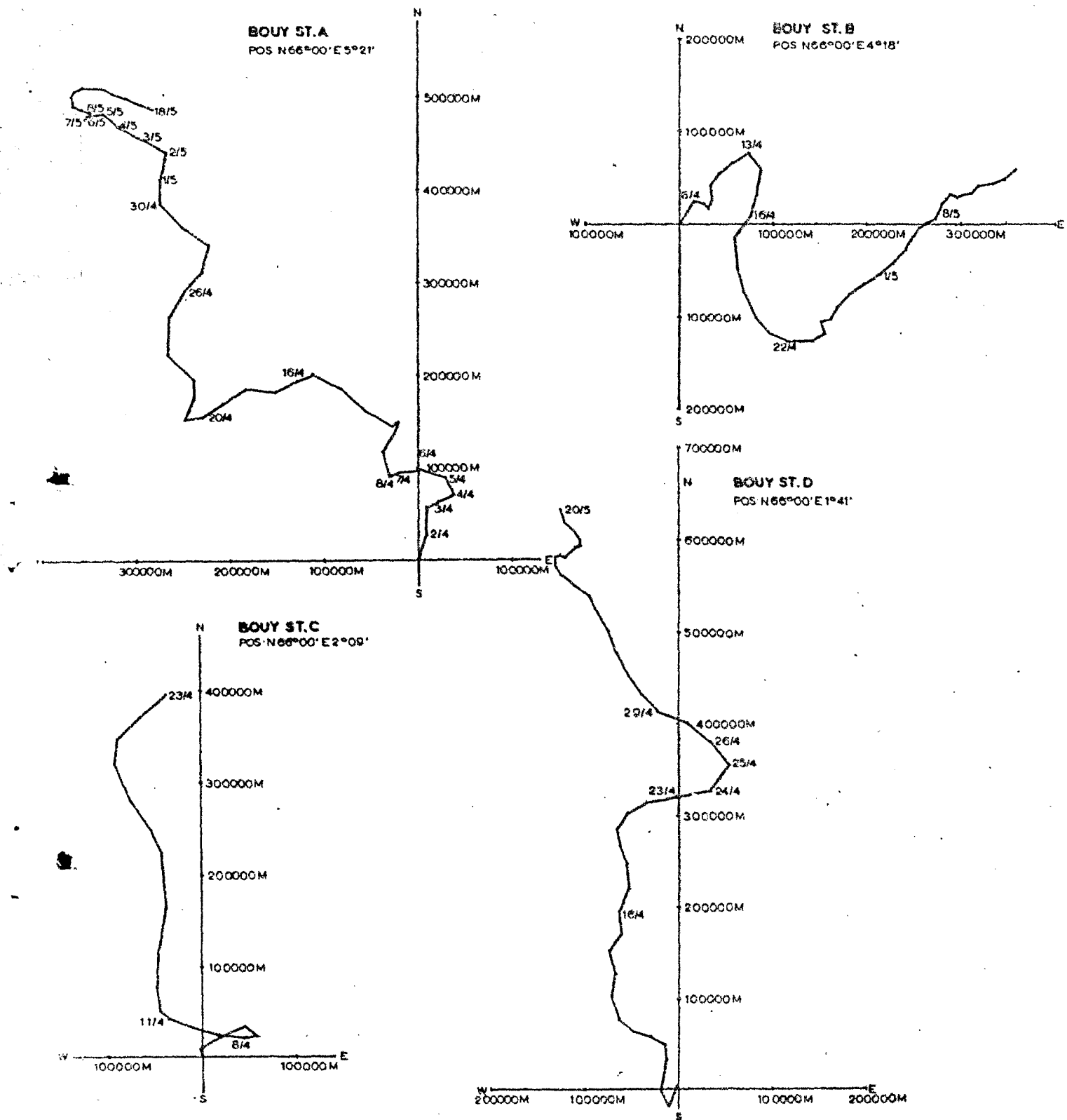


Fig. 18(a): Buoy stations A, B, C and D. Hodographs based on daily mean currents.

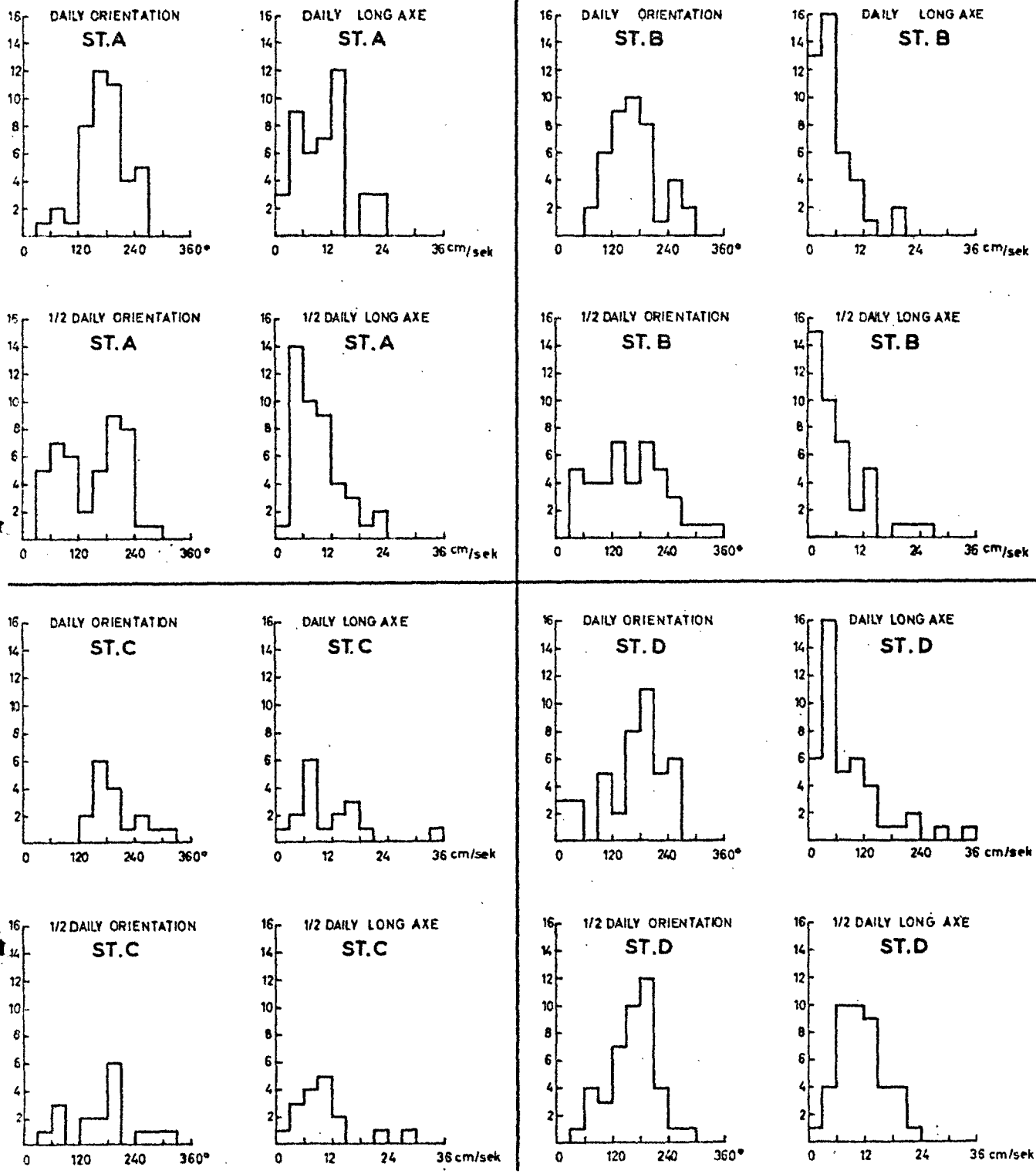


Fig. 18(b): Buoy stations A, B, C and D; histograms of the length of the long axes and the orientation of diurnal and semidiurnal current ellipses.

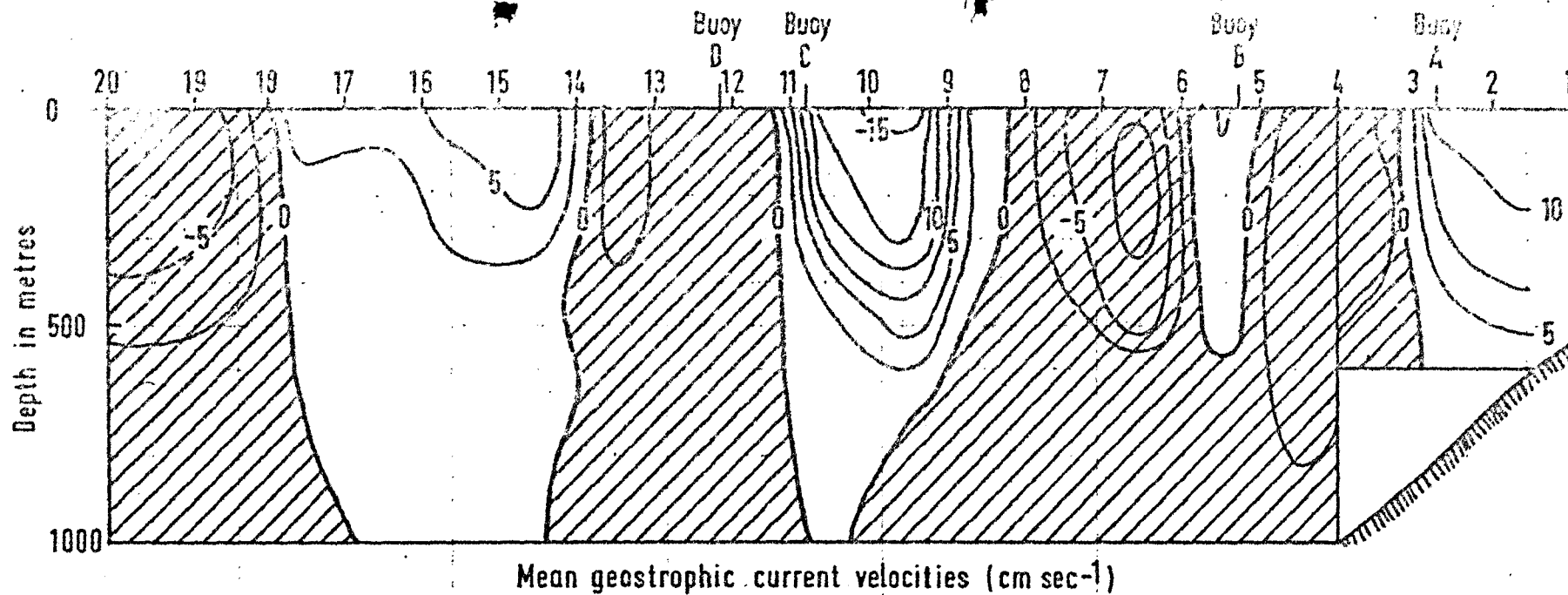


Fig. 19: 66°N Section: Mean N/S geostrophic velocity (cm/sec<sup>-1</sup>): 4 April-18 May 1967. The unshaded areas have a north-going flow and the shaded areas a south-going flow.

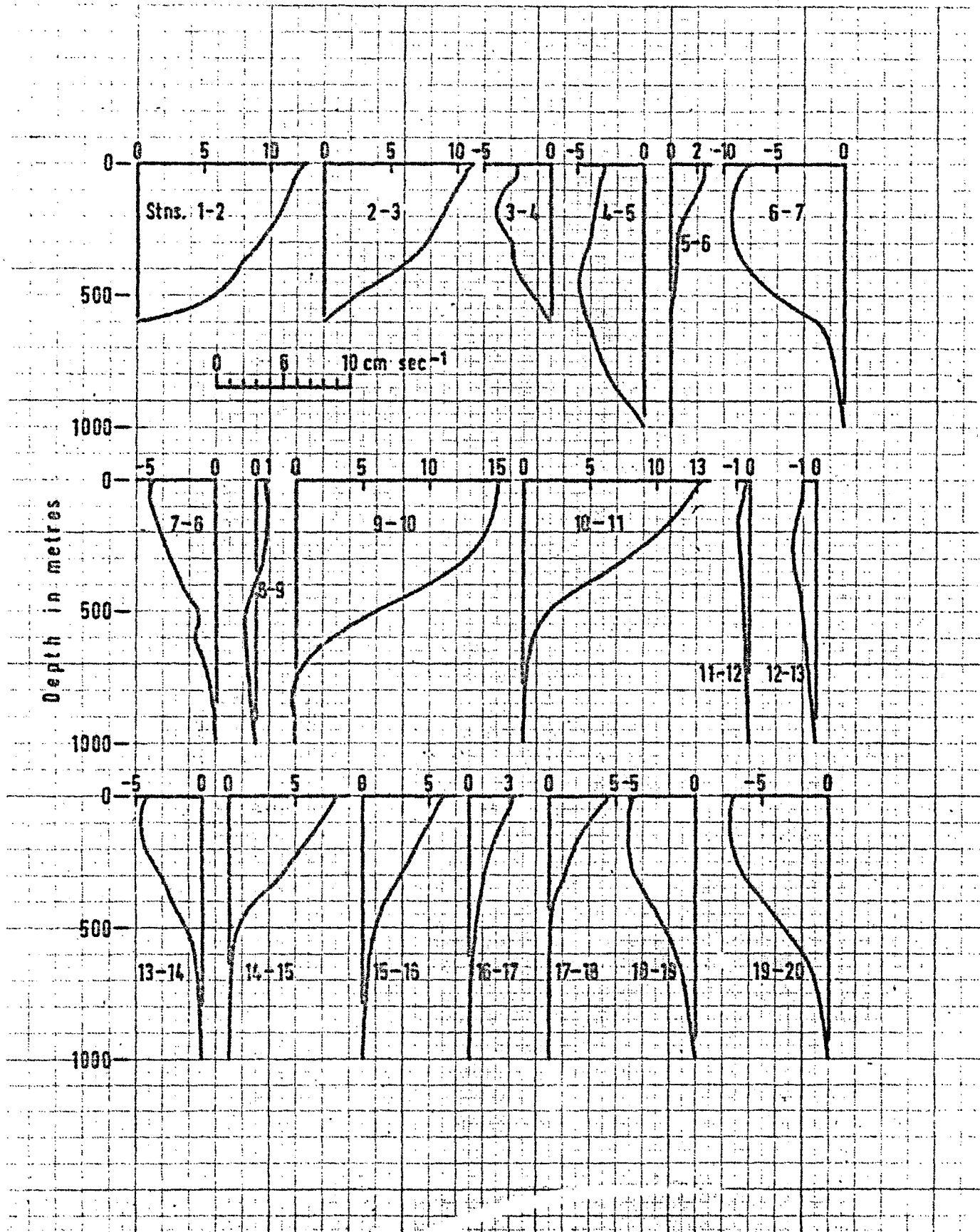


Fig. 20: Stations 1-20: Mean N/S geostrophic velocity profiles: 4 April-18 May 1967. Positive velocities are north-going and negative south-going.



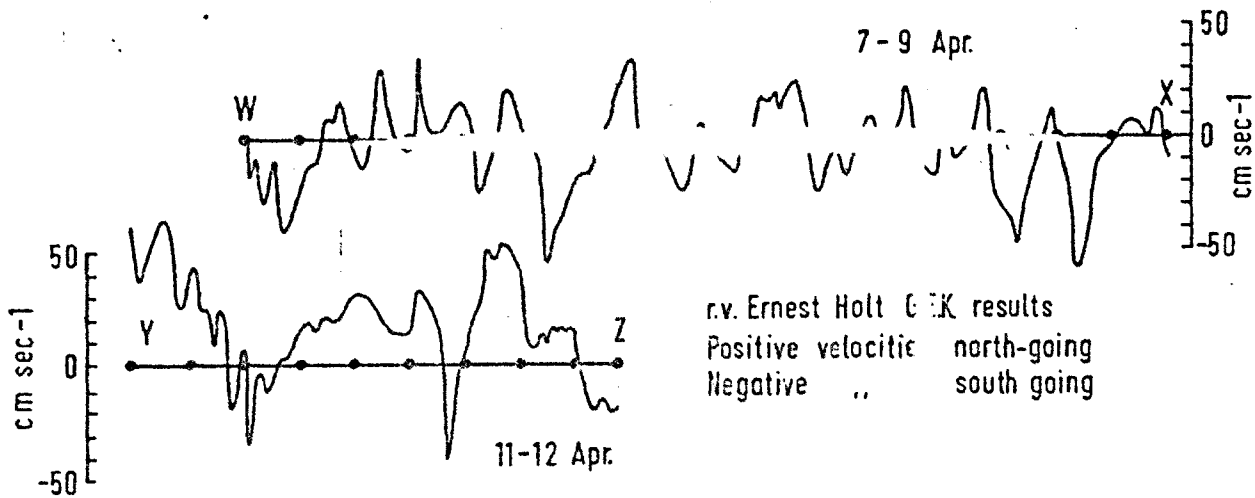
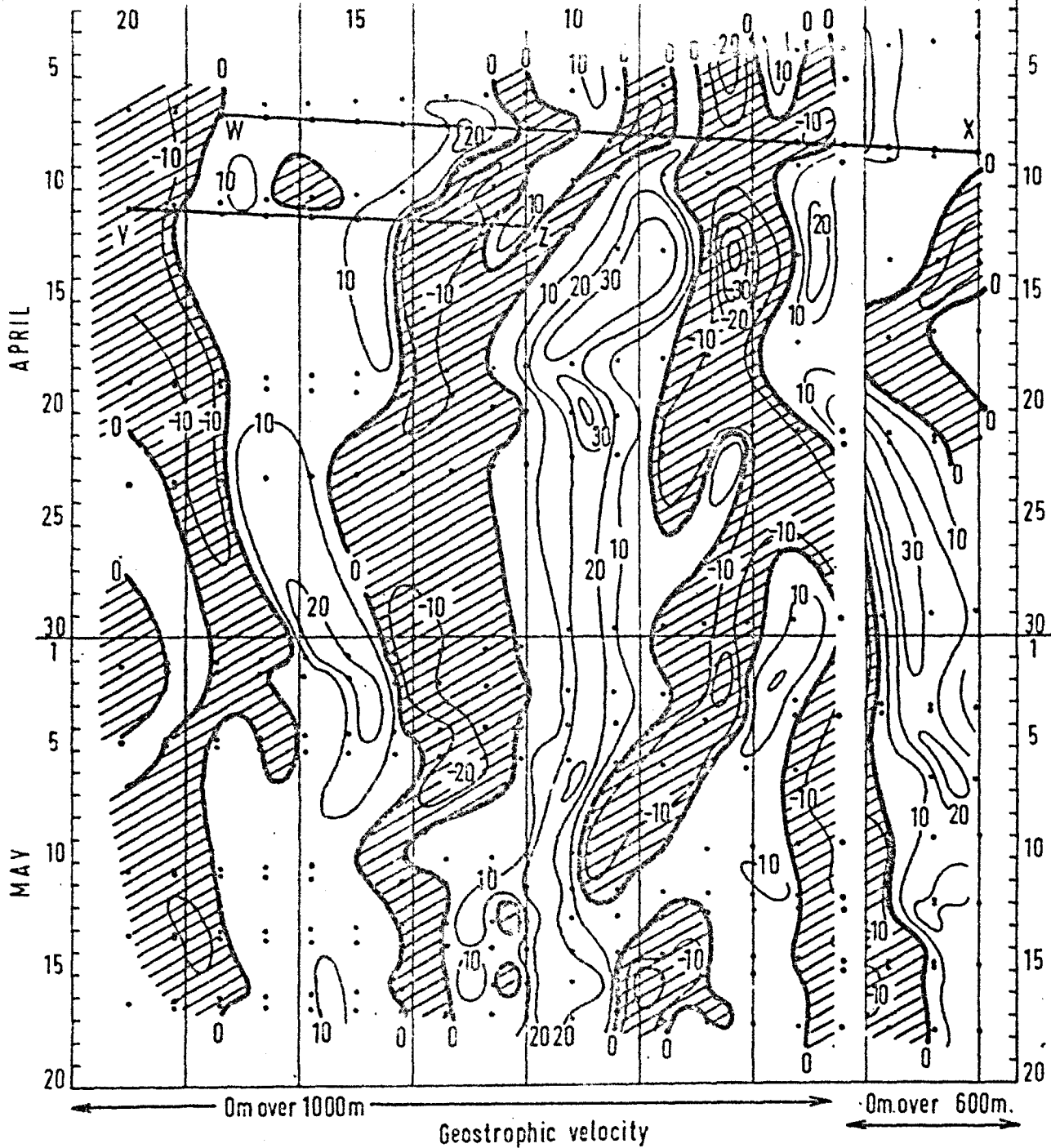


Fig. 21: 66°N Section: Om: N/S geostrophic velocity (cm/sec<sup>-1</sup>): 4 April-18 May 1967 Shaded areas have a south-going flow. The GEK recds obtained on crossings Nos. 2 and 4 are also shown.

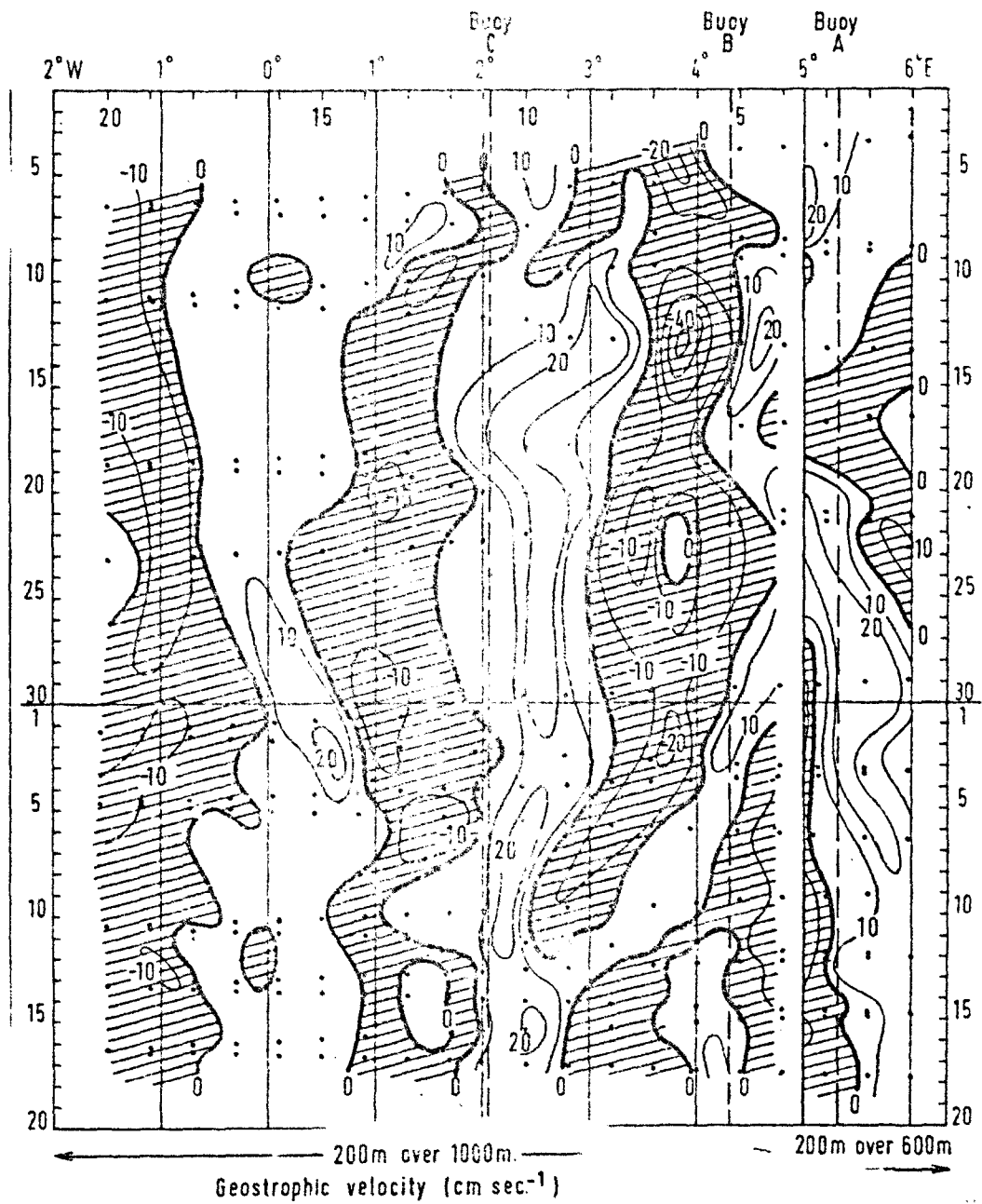


Fig. 22: 66°N Section: 200 m: N/S geostrophic velocity (cm/sec<sup>-1</sup>): 4 April-18 May 1967: Shaded areas have a south-going flow.

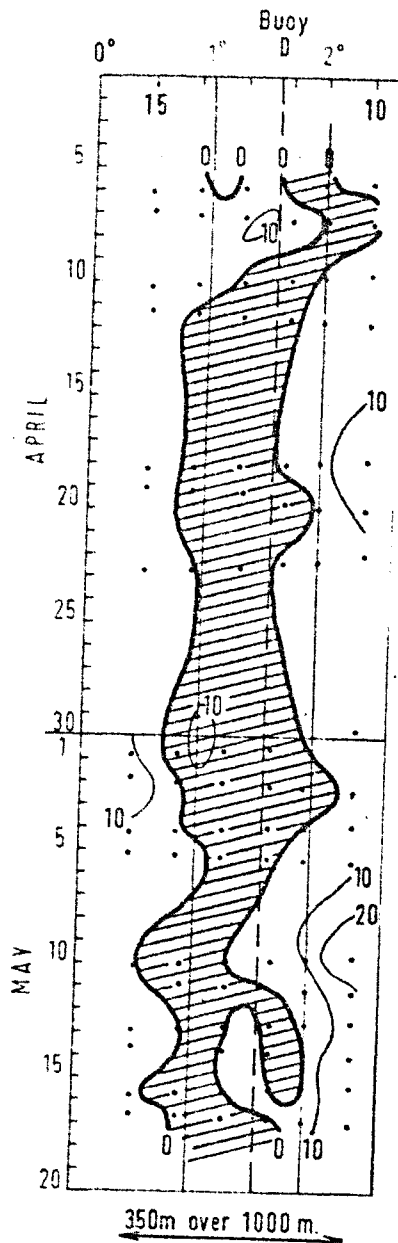


Fig. 23: 66°N Section: 350 m: N/S geostrophic velocity (cm/sec<sup>-1</sup>): 4 April-18 May 1967: Shaded areas have a south-going flow.

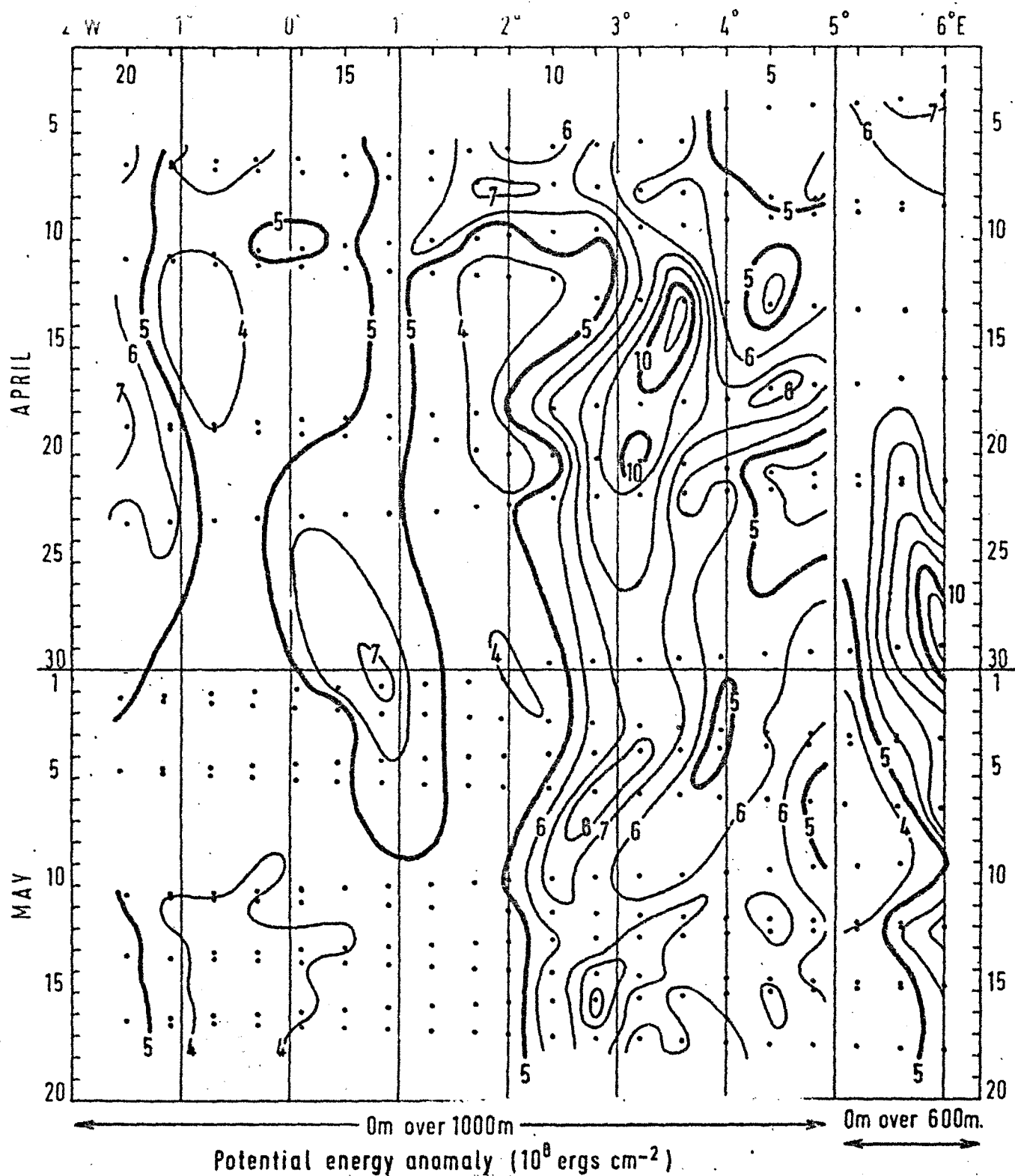


Fig. 24(a):  $66^\circ\text{N}$  Section: Om: Potential energy anomaly: 4 April-18 May 1967: The mass transport normal to the section between 0 and 1000 m depth and between successive isopleths equals  $0.75 \times 10^6$  tonnes  $\text{sec}^{-1}$ . If the isopleth with the higher number is to east the flow is north-going: if it is to the west the flow is south-

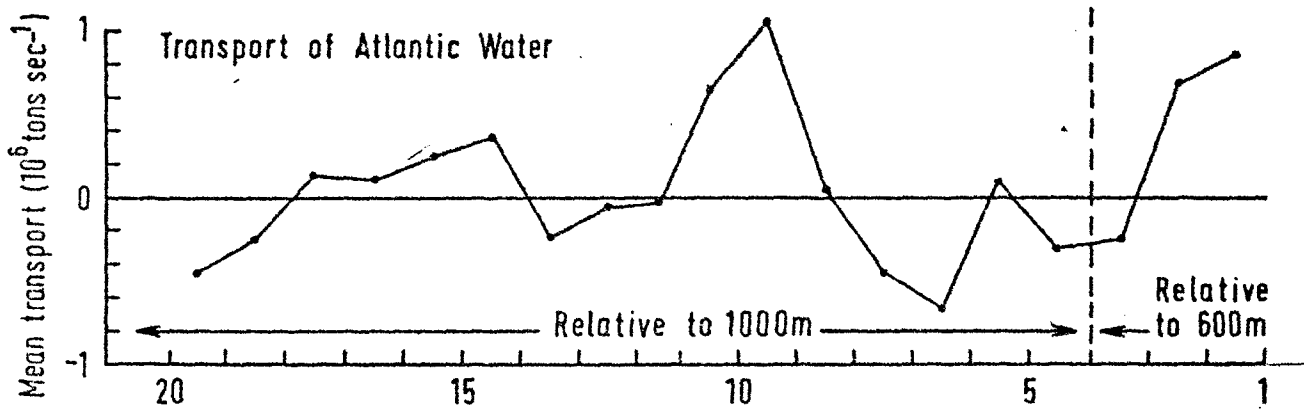


Fig. 24(b):  $66^{\circ}\text{N}$  Section: Mean mass transport of Atlantic water ( $10^6$  tonnes  $\text{sec}^{-1}$ ): 4 April-18 May 1967.

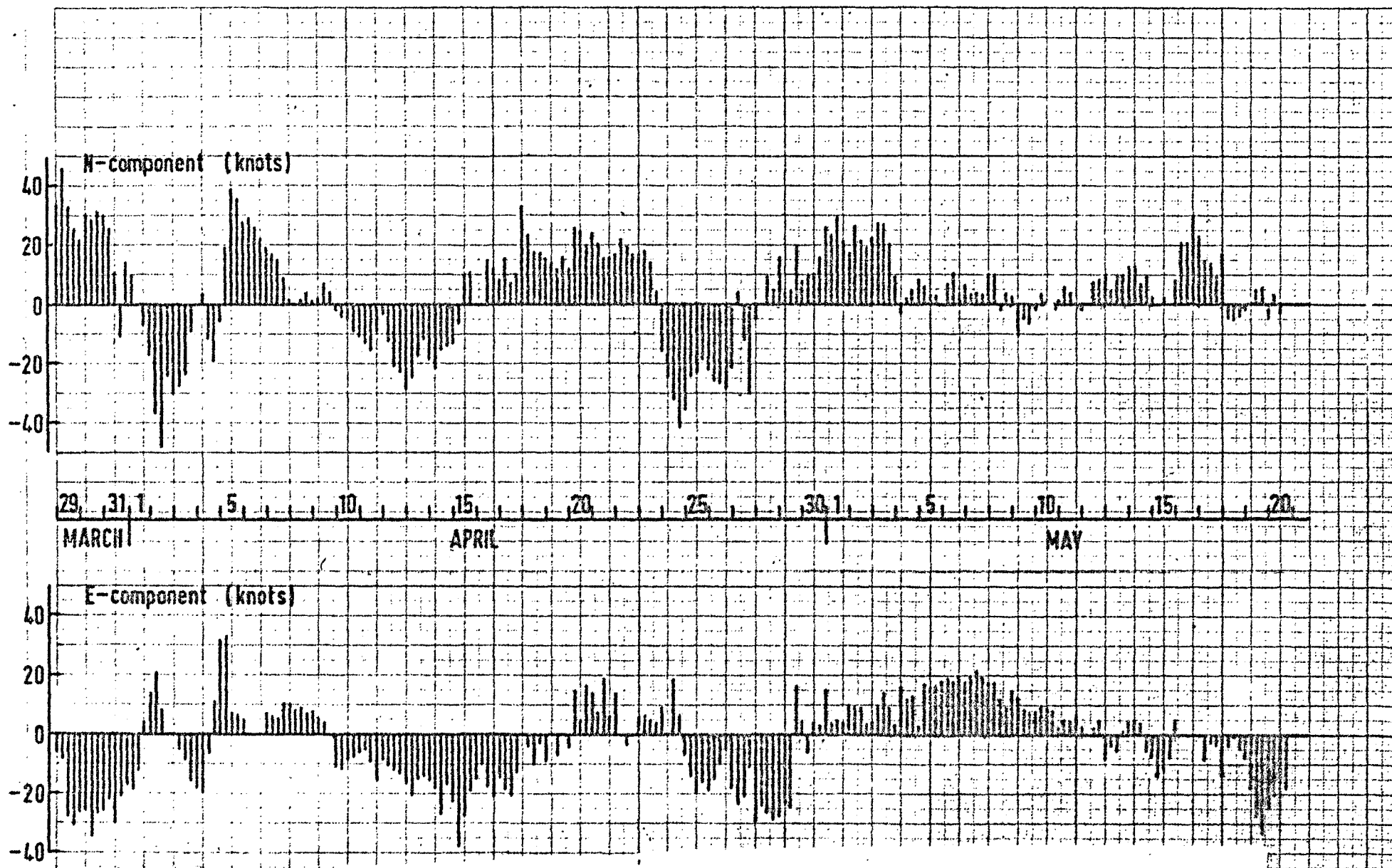


Fig. 25: Ocean Weather Stations METRO: Mean daily north and east wind components: 29 March-20 May 1967.

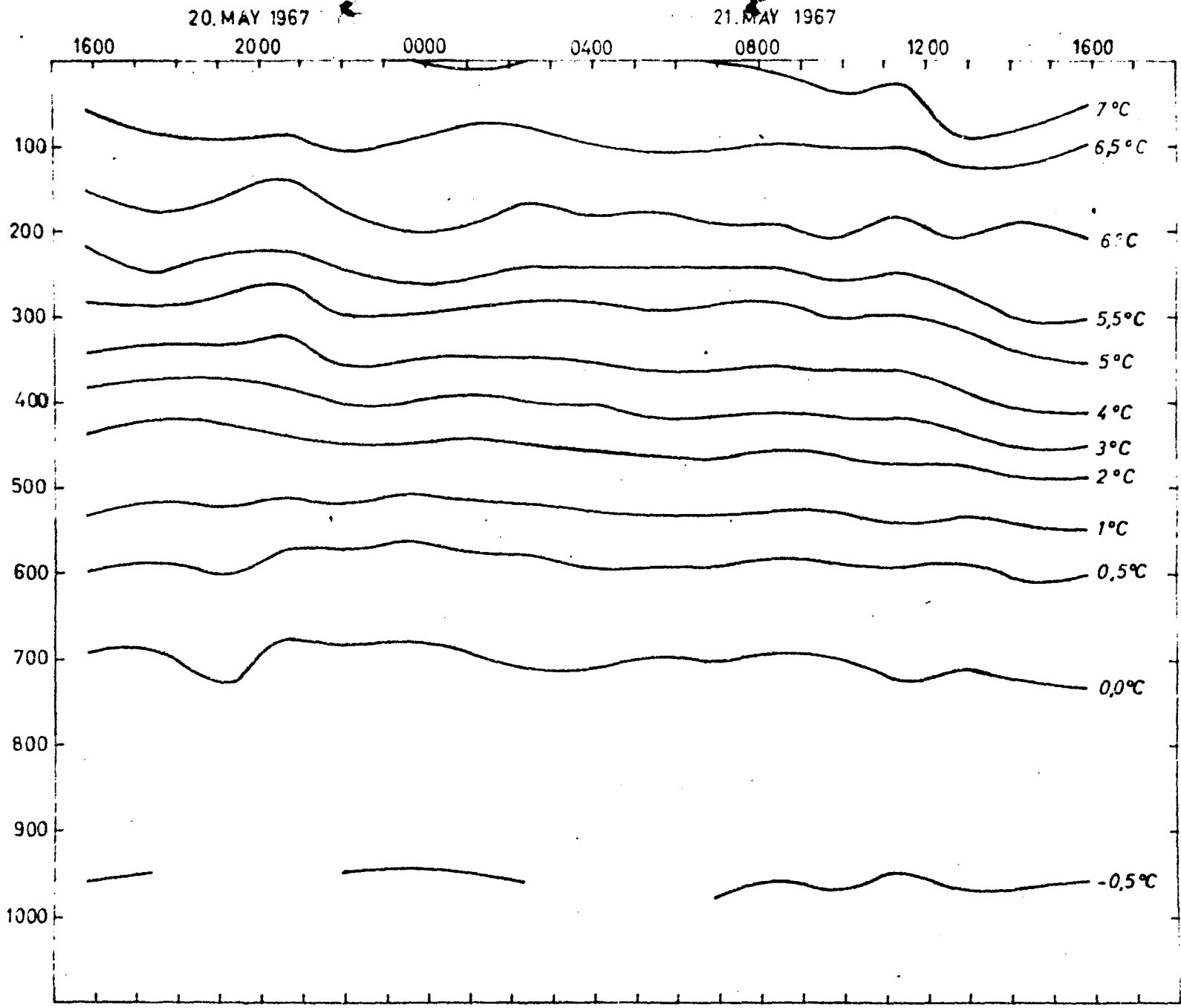


Fig. 26: Position 11. (Near buoystation C) depth of isotherms.